scientific reports

OPEN

Impact of high-fructose diet and metformin on histomorphological and molecular parameters of reproductive organs and vaginal microbiota of female rat

Mürşide Ayşe Demirel[1]✉, Esra Şumlu[2], İbrahim Hanifi Özercan[3], Kazım Şahin[4], Mehmet Tuzcu[5], Veysel Bay[6], Öznur Ece Durmaz Kurşun[7], Mecit Orhan Uludağ[8] & Fatma Akar[9]

There are limited data on the effects of a high-fructose diet on the female reproductive system. Although metformin has some functional effects on female fertility, its reproductive outcome on high fructose diet-induced metabolic syndrome is unclear. The aim of the present study is to evaluate the impact of a high fructose diet on histomorphological and molecular parameters of the reproductive organs and vaginal microbiota as well as the treatment potential of metformin. Wistar albino rats were used in the study. The metabolic syndrome model was induced by a high-fructose diet in rats for 15 weeks. Metformin was orally administered once a day for the last 6 weeks. The high-fructose diet increased blood glucose, triglycerides, insulin, and ovarian testosterone levels; however, it reduced ovarian aromatase levels and follicle numbers and caused uterine inflammation. The high-fructose diet-induced molecular abnormalities on ovarian tissue were demonstrated by the downregulation of ovarian insulin signaling pathway proteins and dysregulation of ovarian mitogenic and apoptotic pathway proteins. A high-fructose diet caused vaginal dysbiosis, metformin increased probiotic bacteria in the vaginal microbiota. Our results revealed that metformin improves ovarian impairments by modulating hormonal balance, insulin level, mapk, and apoptotic signaling molecules, as well as regulating the vaginal microbiota.

Keywords High-fructose diet, Signaling pathways, Metformin, Ovarian tissue, Vaginal microbiota

Metabolic syndrome (MetS) is defined as a pathological condition characterized by abdominal obesity, insulin resistance, hyperglycemia, hyperlipidemia, hypertension, inflammation, and fatty liver. These metabolic features commonly predispose individuals to risk of type 2 diabetes, cardiovascular diseases, and mortality[1,2]. Excess fructose consumption has been linked to an increase in the incidence of insulin resistance and diabetes. Insulin resistance is critical in the pathophysiology of MetS. Moreover, dietary high fructose induces oxidative stress, which leads to increased release of proinflammatory cytokines and, eventually, MetS[3–5]. It is known that MetS is associated with infertility both in men[6–10] and women[8,9,11–14]. A study in male rats revealed that dietary high fructose increases inflammation, damages the blood-testicular barrier, and causes testicular degeneration by upregulation of mitogenic and apoptotic pathways[15]. Previous studies in female rats have shown that MetS is

[1]Department of Basic Pharmaceutical Sciences, Faculty of Pharmacy, Laboratory Animals Breeding, and Experimental Researches Center, Gazi University, Etiler, Ankara 06330, Turkey. [2]Department of Medical Pharmacology, Faculty of Medicine, KTO Karatay University, Konya, Turkey. [3]Department of Pathology, Medicine Faculty, Health Sciences Institution, University of Firat, Elazig, Turkey. [4]Department of Animal Nutrition, Faculty of Veterinary Medicine, Firat University, Elazig, Turkey. [5]Department of Biology, Faculty of Science, Firat University, Elazig, Turkey. [6]Department of Animal Science, Faculty of Agriculture, Ege University, 35100 İzmir, Turkey. [7]Department of Pharmacology, Faculty of Pharmacy, Firat University, Elazig, Turkey. [8]Department of Clinical Pharmacy, Faculty of Pharmacy, Near East University, Nicosia, Turkey. [9]Department of Pharmacology, Faculty of Pharmacy, Gazi University, Ankara, Turkey. ✉email: aysedemirel@gazi.edu.tr

strongly related to polycystic ovary syndrome, which consists of ovulation dysfunction and hyperandrogenism[16,17]. Further studies demonstrated that MetS can also adversely affect pregnancy, as well as embryo development[18,19].

The term "microbiota" describes all microorganisms that live in a defined environment such as skin, mouth, gut, and vaginal tracts, etc. Microbial populations in symbiosis with the host contribute to homeostasis and regulate immunity. Recent studies have shown that microbiota can be associated with health and diseases such as cancers, diabetes, and neurological disorders. Therefore, it has been reported that the regulation of the microbiota may play an important role in the treatment of many diseases[20–22]. The vaginal microbiota is a sensitive microenvironment that changes with hormonal status and diet[23]. In recent years, it has been reported that an imbalance in the vaginal microbiota has been associated with infertility, and the regulation of vaginal microbiota may be effective in its treatment[24–26]. It is known that alterations in dietary patterns may impact the composition and diversity of the vaginal microbiota[27,28]. However, until now, no study has shown the effect of a high-fructose diet on vaginal microbiota.

Several studies have demonstrated the potential of metformin, an oral antidiabetic agent, to enhance ovarian function[29–31]. Metformin improved ovarian angiogenesis and reduced cyst formation by decreasing serum insulin levels in dehydroepiandrosterone-treated mice[32]. Moreover, metformin exhibited a partial restorative effect on androgen-induced proliferation and follicular dynamics of theca cells in female rats administered testosterone[33]. A recent investigation demonstrated that both metformin and exenatide have beneficial effects on the estrus cycle, ovarian morphology, and hyperandrogenemia in rats with insulin resistance and polycystic ovary syndrome (PCOS)[34]. There is evidence that metformin regulates the insulin signaling pathway[35,36] and apoptosis[37–39]. The exact mechanism underlying the therapeutic effects of metformin, which includes the reduction of hyperandrogenism and the induction of ovulation, remains unclear.

The effect of dietary high fructose on the female reproductive system has been less investigated than the males in both animal and human studies[40–42]. Here, we hypothesize that a high fructose diet negatively affects ovarian tissue by disrupting the vaginal microbiome. Metformin may alleviate the insulin signaling pathway and apoptosis mechanisms in ovarian tissue by regulating the vaginal microbiota. The aim of the present study is to investigate the effects of metformin on vaginal microbiota, serum, and ovarian tissue hormone levels, some insulin signaling and apoptosis pathway parameters in ovarian tissue, and the related histopathological mechanisms in female rats with high fructose-induced metabolic syndrome. According to our literature search, no comprehensive study targets these mechanisms impaired by a high-fructose diet. Our results targeting multiple mechanisms may contribute to understanding the complex relationship between vaginal microbiota and high fructose diet-induced MetS as well as the therapeutic potential of metformin.

Materials and methods
Chemicals and drugs
Fructose was obtained from Danisco Sweeteners, Finland. Xylazine hydrochloride (Xylazin Bio® 2%) and ketamine hydrochloride (Ketasol® 10%) were purchased from Interhas, Turkiye. Glucose, triglyceride, total cholesterol, low-density lipoprotein (LDL) cholesterol, and high-density lipoprotein (HDL) cholesterol kits were from BioVision, USA. The insulin kit was purchased from Cusabio, Wuhan, China. Aromatase, estrogen, progesterone, testosterone, and inhibin kits were bought from USCN, Wuhan, China. Estrogen, progesterone, and testosterone immunohistochemistry antibodies were Roche Diagnostic, Germany. Insulin Receptor Substrate (IRS)-1, protein kinase B (Akt), and endothelial NOS (eNOS) polyclonal antibodies were from Bioss-USA. Protein bands were visualized using an enhanced chemiluminescent reagent (ECL) of ClarityTM, BioRad Laboratories. Total RNA isolation kits from Qiagen, Venlo, Holland and cDNA synthesis kit from Thermo Scientific, USA were purchased. For gene expression of *irs-1, akt, enos, mitogen-activated protein kinase (mapk), extracellular-regulated kinase (erk) 1/2, C-Jun N-terminal kinase (jnk), B-cell lymphoma (Bcl)-2, Bcl-2-associated X protein (Bax)*, and *caspase-3*, bright-green 2X qPCR MasterMix-No Dye was purchased from ABM Good, Canada. SYBR Green Mastermix was purchased from Roche, Germany.

Animals
Three-week-old female, healthy, 28 Wistar albino rats weighing 75–85 g were provided from Kobay Experimental Animals Laboratory Inc., Ankara, Turkey. The study was conducted under the ARRIVE (Animal Research: Reporting of In Vivo Experiments) guidelines. All experimental procedures were performed according to NIH guidelines for housing and care of laboratory animals and approved by the Experimental Animal Ethics Committee of Gazi University (G.Ü.ET-18.084). The animals were kept in polysulfone cages (3 rats per cage; 425×266×185 mm in size) with aspen shavings for bedding at 21–24 °C, 40–45% humidity, and light-controlled (12 h light/12 h dark) conditions at Laboratory Animal Care and Research Unit, Faculty of Pharmacy, Gazi University (Ankara, Turkiye). Rats were fed with a standard pellet diet (5.5% fat, 23% proteins, 3.5% cellulose, 8% ash, 11% NDF; 12.5 kJ/g) and water *ad libitum* throughout the experimental procedure. The rats' weights were recorded weekly during the experimental procedure.

Induction by high fructose diet of rat metabolic syndrome model
A flow chart of the experimental procedure is given in Fig. 1. After 1 week of acclimation, rats were randomly divided into four groups as follows: control (C; *n*=6), fructose (F; *n*=8), metformin (M; *n*=6), and fructose+metformin (F+M; *n*=8). Metabolic syndrome was induced by adding 20% fructose solution (w/v) to drinking water, prepared daily, for fifteen weeks[43]. The C and M groups were not subjected to the metabolic syndrome model.
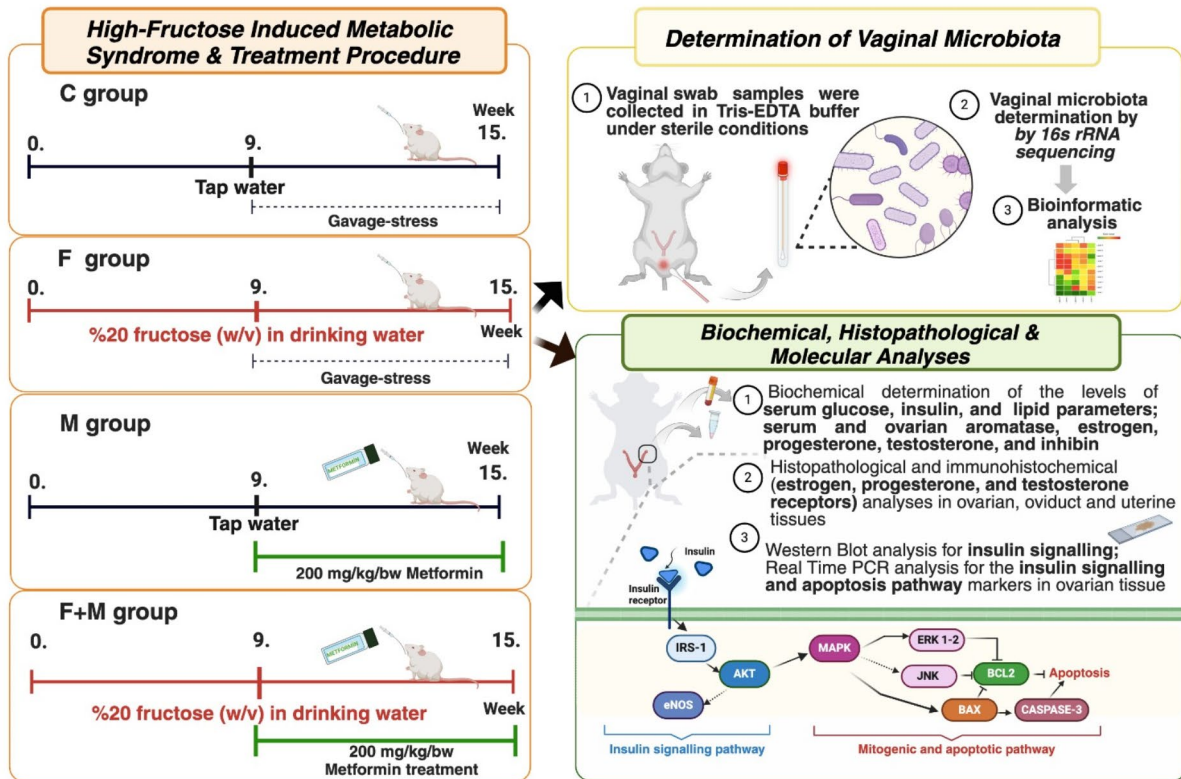
Fig. 1. Flow chart of the experimental procedure (Created with BioRender.com).

Treatment procedure

Metabolic syndrome was treated with metformin for the final 6 weeks. The C and F group's rats received no treatment; instead, only gavage was given to them to induce gavage stress. The M and F + M groups were treated with metformin. Metformin was administered at 200 mg/kg doses[44] by oral gavage (1 mL *per* rat, daily).

Termination of the experimental procedure

At the end of the experimental procedure, samples were collected from the vagina of the rats for monitoring of the vaginal microbiota profile. For sampling, the swab was inserted into the vagina under sterile conditions and then taken into tubes. All swab samples were stored at − 80 °C (Sanyo®) until DNA extraction. All the rats were sacrificed by taking blood from the heart under general anesthesia (10 mg/kg xylazine hydrochloride and 80 mg/kg ketamine hydrochloride). Blood samples were centrifuged for 15 min at 3,000 rpm (ZIP IQ L Scientific) to separate serum and subsequently stored at − 80 °C until analysis. The uterine and ovarian tissues were dissected and stored under suitable conditions for analysis.

Biochemical parameters

Serum

Serum glucose, triglyceride, total cholesterol, LDL cholesterol, HDL cholesterol, insulin, aromatase, estrogen, progesterone, testosterone, and inhibin concentrations were assayed by enzyme-linked immunosorbent assay (ELISA; Azure Biosystems Microplate Reader) using a commercial rat kit according to the manufacturer's instructions.

Tissue

Ovarian tissue samples were homogenized using a homogenizer (Tissue RuptureTM, Qiagen, USA). Homogenization of the ovarian tissue was carried out in a medium composed of 50 mM phosphate buffer (pH: 7.4). For each sample, 0.5 g tissue was homogenized in a 4.5 mL working solution. The homogenate was centrifuged at 3,000 rpm for 5 min, and supernatants were collected to measure estrogen, progesterone, testosterone, and aromatase levels. Analyses were evaluated using ELISA kits according to the manufacturer's instructions.

Protein expressions by western blot in the ovarian tissue

Ovarian samples were frozen with liquid nitrogen and stored at -80°C. The tissues were homogenized (Tissue RuptureTM, Qiagen, USA) in a solution containing Tris 50 mM (pH 7.4), NaCl 150 mM, EDTA 5 mM, 1% v/v Triton X-100, 0.26% (w/v) sodium deoxycholate, 50 mM sodium fluoride, 0.1 mM sodium orthovanadate and 50 µg/ml phenylmethylsulfonyl fluoride (Tissue RuptureTM, Qiagen, USA). And then, it was centrifuged at 12,000 x g for 3 min at 4 °C to remove unwanted cell debris[45]. Total protein concentrations in the nuclear and cytoplasmic fractions were determined according to Lowry's method[46]. Expressions of IRS-1, Akt, and eNOS proteins, associated with the insulin signal transduction pathways, were measured in ovarian tissue samples. Accordingly, the proteins of ovarian tissues were separated from each other by the SDS-PAGE method and transferred to the PVDF membrane (blotting). Western Blot membranes were washed with TBST (0.5 M NaCl, 20 mM Tris pH: 7.4, 0.05% v/v Tween-20) and were blocked with 5% bovine serum albumin (prepared in TBST) for one hour. Blocked membranes were labeled with primary antibodies overnight at room temperature. After excess antibodies were washed with TBST, secondary antibodies which were conjugated with horseradish peroxidase (HRP) were applied for 1 h. The blots were then incubated with an ECL for 5 min, and the bands' images were scanned with a chemiluminescence imaging device (ChemiDoc™ MP, Bio-Rad, USA). Band intensities were determined with the Image Lab4.1 Program. Blots were also probed for GAPDH proteins as loading controls, and the experiments were repeated at least three times.

Irs-1, *akt*, *enos*, *mapk*, *erk 1/2*, *jnk*, *bax*, *bcl-2*, and caspase-3 gene expression on ovarian tissue

The mRNA expressions of genes associated with the insulin signaling pathway (*irs-1*, *akt*, *and enos*), MAPK pathway (*mapk*, *erk 1/2*, *jnk*), and apoptosis (*bax*, *bcl-2*, *caspase-3*) were carried out on ovarian tissues. Total RNA was extracted from each tissue using RNeasy total RNA isolation kits according to the manufacturer's instructions. The amount and purity of total RNA were spectrophotometrically measured at a 260/280 nm ratio. Total RNA was reverse transcribed into cDNA using the commercial first-strand cDNA synthesis kit. According to the method, 1 µl of oligo(dT)15 primer (100 µM) was added to 1 µg of total RNA, then the total volume was made up to 12 µl with nuclease-free DEPC water. After adding 4 µl of 5x M-MuLV reaction buffer, 1 µl of RiboLockTM (20 µ/µl) (Fermentas, USA), and 2 µl of 10 mM dNTP mixture, the tubes were incubated at 37 °C for 5 min. Then, 1 µl of M-MuLV RT (200 u/µl) was added, and the cDNA synthesis reaction was carried out with a thermal cycler (Bioneer, South Korea) for 1 h at 42°C. For reverse transcriptase denaturation, cDNA samples were kept at 70 °C for 5 min and cooled on ice. The samples were stored at – 80 °C until qRT-PCR studies. The mRNA amount of these genes was measured using SYBR Green I reaction chemistry and a quantitative real-time polymerase chain reaction (qPCR). Primer design for the target gene was determined using the Perl Primer program. The primer sequences of the gene are shown in Table 1. For qRT-PCR, 1 μl of cDNA was mixed with forward and reverse primers (2 µM of each primer) and 5 µl SYBR Green Mastermix. The thermal cycling conditions were as follows: initial denaturation at 95 °C for 10 min, denaturation at 94 °C for 15 s, annealing at 58 °C for 30 s, and extension at 72 °C for 30 s followed by 40 cycles. Fluorescence was determined by the LightCycler 480 II instrument (Roche, Germany). Each experiment was carried out with each sample in triplicate. Expression levels of the target genes were normalized to the mRNA level of GAPDH as a reference gene. The $2^{-\Delta\Delta CT}$ method was used to calculate the relative expression level of each gene.

The histopathological investigation

Ovarian, oviduct and uterine horn tissues were fixed in Bouin's solution for 12 h. The tissues were dehydrated in graded ethanol (75, 96, and 100%). After permeation in xylene, they were embedded in paraffin using standard procedures. Then sections were cut to a thickness of 4 µm by microtome (Leica, Germany). One of each paraffin block was stained with Hematoxylin&Eosin. The other three sections were stained by the immunohistochemical method. The slides were blindly examined by a pathologist using an Olympus BX52 microscope (Olympus Co., Tokyo, Japan).

Gene	Forward primer (5′ to 3′)	Reverse primer (5′ to 3′)
bax	AGGGTTTCATTCCAGGATCGAGC	AGGCGGTGAGGACTCCAGCC
bcl-2	CGGGAGAACAGGGTATGA	CAGAGACAGCCAGGAGAA
caspase-3	GACTGCGGTATTGAGACAGA	CGAGTGAGGATGTGCATGAA
irs-1	GCCAATCTTCATCCAGTTGC	CATCGTGAAGAAGGCATAGG
akt	GTGGCAAGATGTGTATGAG	CTGGCTGAGTAGGAGAAC
enos	CGAGATATCTTCAGTCCCAAGC	GTGGATTTGCTGCTCTCTAGG
mapk	AGGGCGATGTGACGTTT	CTGGCAGGGTGAAGTTGG
erk1/2	TCAAGCCTTCCAACCTC	GCAGCCCACAGACCAAA
jnk	AACTCTTTGACGCTGCTTGC	TGAAGCACTGTGCCTTTACC
gapdh	GATTGTTGCCATCAACGACC	GTGCAGGATGCATTGCTGAC

Table 1. Primer sequences.

Evaluation of ovarian, oviduct, and uterine horn tissues under the light microscope
The ovarian, oviduct, and uterine horn tissue samples of a rat were placed in the same tissue cassette. Perpendicular sections were taken from the full-thickness uterine wall and embedded in paraffin. In each specimen, 5 serial sections of 4 μm were obtained. The presence of inflammation in the ovarian, oviduct, and uterine horn tissues was scored as no (score: 0), mild (score: 1), moderate (score: 2), and severe (score: 3)[47]. The assessment was conducted on the endometrial glands, stromal components in the uterine horn, and the epithelium and stroma in the oviduct. Additionally, the evaluation of ovarian follicular activity involved recording the numbers of primary, secondary, and tertiary follicles and the corpus luteum in ovarian tissues.

Immunohistochemical analysis
Immunohistochemical staining was performed using the streptavidin-biotin peroxidase method to determine estrogen, progesterone, and testosterone receptor antibodies in the ovarian, oviduct, and endometrium tissues. Four μm thick sections were deparaffinized and placed on polylysine-coated glass slides. The slides were subjected to a deparaffinization process for 30 min at 65–70 °C in an incubator. Then, all slides were loaded in an automated system (Ventana® Ventana Benchmark UltraAutostainer) and labeled with estrogen, progesterone, and testosterone receptor antibodies. The labeled cells were visualized with DAB chromogen (brown), and the background was stained with Mayer's hematoxylin. Immunopositive cells were counted in 5 different microscopic fields at × 200 magnification. Nuclear staining in the stromal and the epithelial cells was considered positive for all antibodies. A semiquantitative method was used to assess the staining degree[48]. The nuclear staining intensity was scored from 0 to 3 (no staining: 0; slightly staining: 1; moderately staining: 2; and strongly staining: 3). The stained cells percentage was scored as 0 to 3 according to the ratio of the number of the cells showing nuclear staining to the total number of the stromal cells or epithelial (no staining: 0; 1 to 33%: 1; 34 to 66%: 2; 67 to 100%:3). Then, the immunohistochemistry score (IHCS) was obtained by multiplying the staining intensity and percentage score[49].

Determination of vaginal microbiota by next generation sequencing method and metagenomic approach

Vaginal swab samples were obtained from rats under sterile conditions at the end of the experimental procedure. The samples were transferred to tubes containing sterile Tris-EDTA (TE) buffer. The samples were stored at – 80 °C until analysis. The solution obtained by rapid mixing in a cold environment for about an hour was centrifuged at 5000 g for 10 min to remove eukaryotic cells. Subsequently, the supernatant was collected and centrifuged at 13,000 g for 15 min. The resulting pellet was then dissolved, and DNA isolations were performed using DNA isolation kits according to the manufacturer's instructions. DNA concentrations were determined using the Qubit 2.0 Fluorometer, and the DNA samples were stored at – 20 °C until use. For the library preparation, PCR was carried out following the guidelines provided by Illumina. Universal primers, 341 F (Illumina_16S_341F 5′-TCG TCG GCA GCG TCA GAT GTG TAT AAG AGA CAG CCT ACG GGN GGC WG CAG), and 805R (Illumina_16S_805R 5′-GTC TCG TGG GCT CGG AGA TGT GTA TAA GAG ACA GGA CTA CHV GGG TAT CTA ATC C) including adapter sequences were used[50] to amplify the V3-V4 hypervariable region of the 16 S rRNA gene.

The quality of PCR products was assessed using the Qubit instrument. After cleaning the PCR products from free primers and primer dimers and calculating the DNA concentration, amplicon libraries were sequenced on a lane of the Illumina® MiSeq platform.

The initial raw data from sequencing was converted into FASTA format. Quality control for the reads was carried out using QIIME 2 software[51]. Reads with Phred scores below 20, primer and barcode sequences, and chimeric sequences were filtered out using DADA2 software[52]. QIIME 2 software was then employed for the taxonomic assignment of each cluster, matching a representative sequence from each Operational Taxonomic Unit (OTU) to a sequence in the GreenGenes database.

Chao1 and Shannon diversity indexes were utilized to assess the richness and evenness of the samples. The comparison of group indexes was conducted through the Kruskal-Wallis test. The beta diversity of the samples was assessed and compared through analysis of the first three principal components (PCs), computed using the ClustVis web tool[53]. The resulting PC values were then visualized in 3D scatterplots using JMP Pro 13. Mean relative abundances of the first ten phyla and twenty genera were charted and compared for each pair of groups.

Following the previously described methods, the microbiota profiles of each group were compared[54,55]. In brief, Log fold changes (Log10) in the relative abundance of genera were computed for each group, and pairwise comparisons were conducted between groups. Robust response screening analysis, carried out in JMP Pro 13 (SAS Institute Inc., Cary, NC), was employed to assess differences in general relative abundance between pairs of groups. A false discovery rate (FDR) correction was applied, and statistical significance was determined at an FDR LogWorth of 1.3 (equivalent to a p-value of 0.05).

Statistical analysis
Statistical analyses were performed using GraphPad Prism 8.0. Results are expressed as the mean ± standard error of the mean (SEM). The one-way ANOVA followed by Dunnett's Multiple Comparison Test was used to determine the significance of differences among groups. Statistical significance was assumed at the level of $p < 0.05$.

Results
The metabolic syndrome model was induced by a 20% fructose diet. When the weekly weight changes of the experimental groups were compared, it was seen that the highest weight gain was in the F group (Fig. 2). At the end of the experimental protocol, this change in the F group was statistically significant compared to the C and
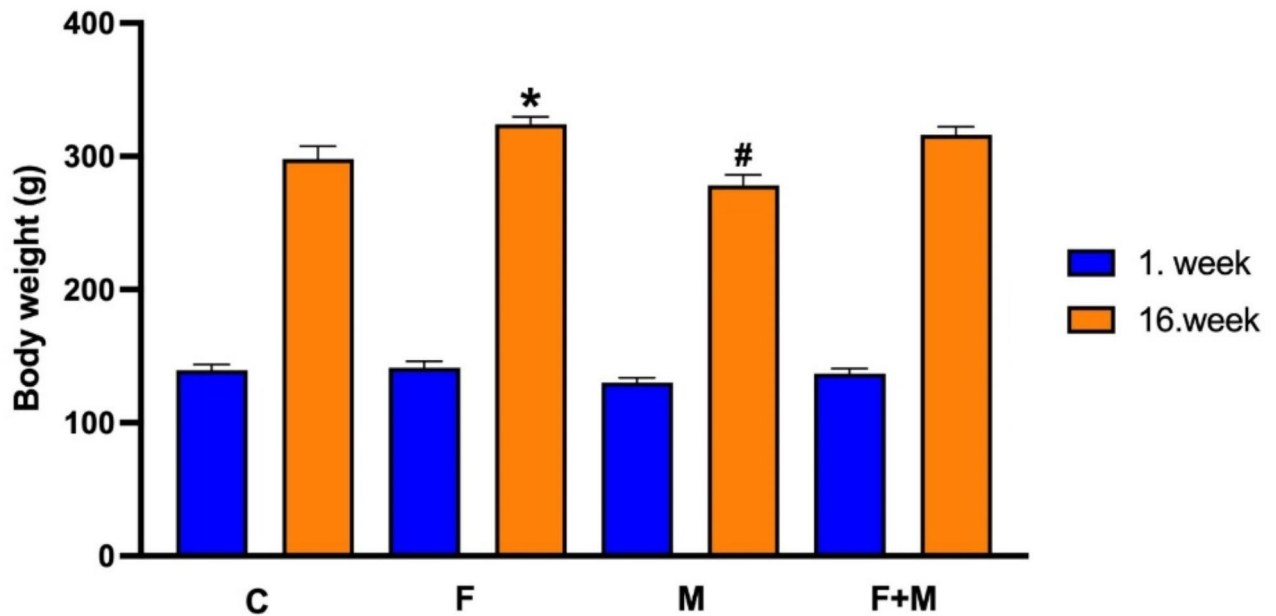
Fig. 2. Body weight changes of rats before and after the experimental procedure. C: Control; F: Fructose; M: Metformin; F + M: Fructose + Metformin. *$p < 0.05$, significantly different from C and M groups; # $p < 0.05$, significantly different from F + M group.

M groups. On the other hand, the lowest weight gain was in the M group and different from the F + M group ($p < 0.05$). However, there was no difference between the F and F + M groups ($p > 0.05$) in terms of weight gain.

The effects of dietary high-fructose and metformin on serum and tissue biochemical parameters

Serum: Serum glucose, insulin, triglyceride, and total cholesterol levels of the F group were found to be higher than the other groups. Serum glucose and triglyceride levels significantly increased in the F group when compared to that of the other groups ($p < 0.05$). Insulin level was increased in the F group as compared to those of the C group ($p < 0.05$). It was observed that serum glucose, triglyceride, and insulin levels were decreased with metformin treatment. However, it was noted that there was no significant difference among the groups in total cholesterol, LDL, and HDL values ($p > 0.05$) (Fig. 3).

When the serum aromatase, inhibin, estrogen, progesterone, and testosterone levels of all groups were compared, it was seen that there was no significant difference among the groups. Nevertheless, a decrease in aromatase and estrogen levels of the M group was found compared to the other groups. Moreover, the testosterone level of the F group increased compared to the other groups (Fig. 4).

Tissue: The levels of tissue biochemical parameters are given in Fig. 5. The testosterone level of ovarian tissue was highest in the F group. This level of the F group was found to be significantly different between the C and the F + M groups ($p < 0.05$). The aromatase level was the highest in the M and C groups. The aromatase levels of the F group and F + M group were found to be decreased compared to the C group ($p < 0.05$). It was also noted that the difference in tissue aromatase levels was significant between the M and the F groups ($p < 0.05$). No significant difference was determined among all the groups in terms of estrogen and inhibin levels of ovarian tissue ($p > 0.05$). Tissue progesterone levels were significantly decreased in the F group compared to the C group ($p < 0.05$). However, the progesterone level of the F + M group was different compared to the M and the F groups ($p < 0.05$).

The effects of dietary fructose and the metformin administration on the protein expression of ovarian insulin signaling pathway parameters

The protein expressions of Akt, eNOS ve IRS-1 in ovarian tissue of rats are given in Fig. 6 as a percentage of control values. It was observed that Akt, eNOS, and IRS-1 protein levels in the ovarian tissues of the F group were significantly decreased compared to other groups ($p < 0.05$). However, it was determined that the levels of these proteins in the ovarian tissues of the F + M group increased significantly when compared to the F group ($p < 0.05$). The Akt protein level in ovarian tissue was seen to increase with the administration of metformin (M group) and the difference among the C, F, and F + M groups was significant ($p < 0.05$).

Insulin signaling, and Mapk pathways; apoptotic gene expression on ovarian tissue

Ovarian insulin signaling pathway (*akt*, *enos*, and *irs-1*); mapk pathway (*mapk*, *erk1/2*, *jnk*); apoptosis-related genes (*bax*, *bcl-2*, *caspase-3*) in ovarian tissues of rats were measured by qRT-PCR. Results are expressed as
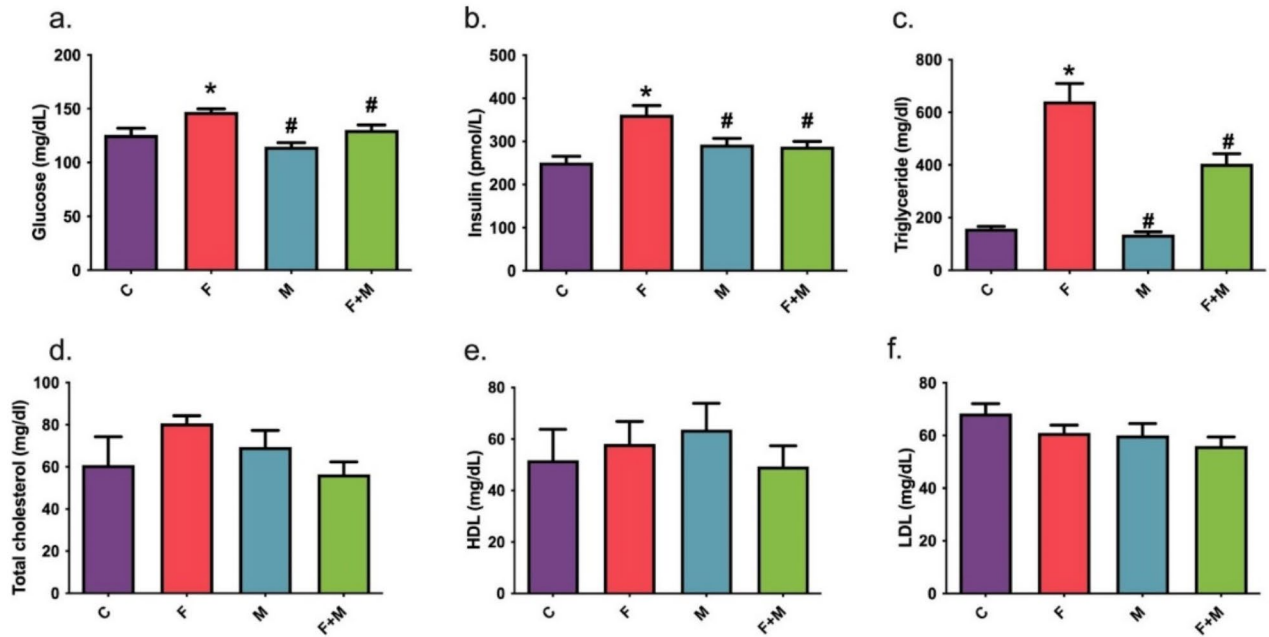
Fig. 3. The serum levels of (**a**) glucose, (**b**) insulin, (**c**) triglyceride, (**d**) total cholesterol, (**e**) high-density lipoprotein, and (**f**) low-density lipoprotein. Each bar represents at least six rats. C: Control; F: Fructose; M: Metformin; F + M: Fructose + Metformin. *$p < 0.05$, significantly different from C group; # $p < 0.05$, significantly different from F group.
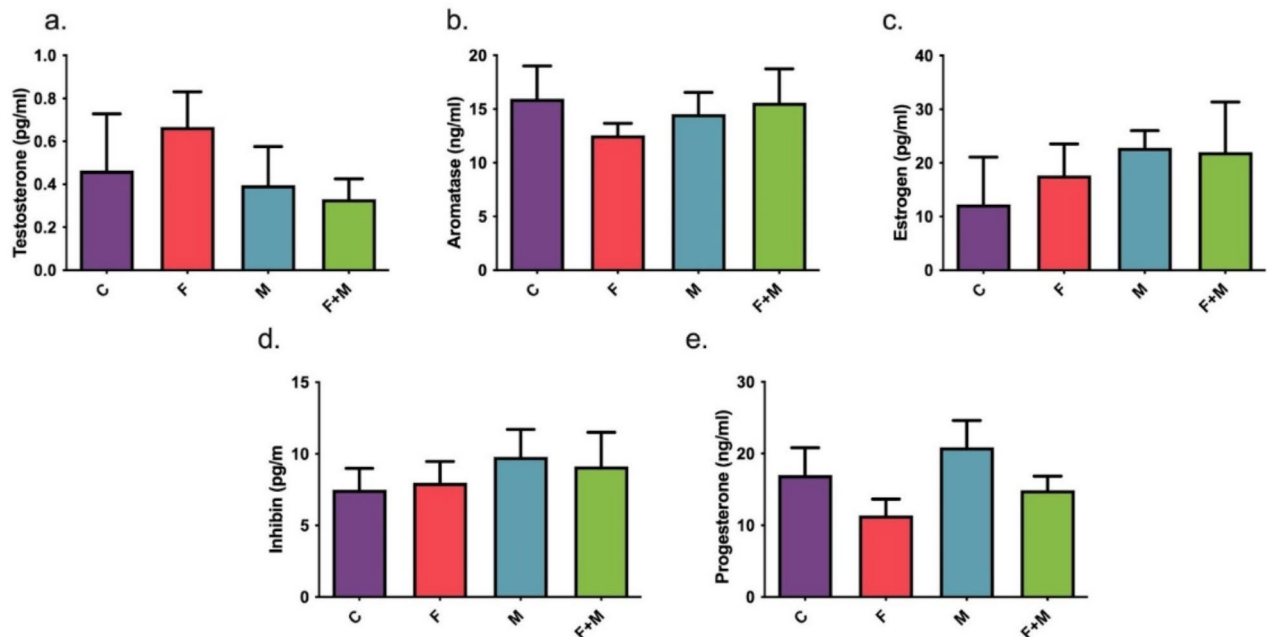

Fig. 4. The serum levels of (**a**) testosterone, (**b**) aromatase, (**c**) estrogen, (**d**) inhibin, and (**e**) progesterone. Each bar represents at least six rats. C: Control; F: Fructose; M: Metformin; F + M: Fructose + Metformin.

fold change (Figs. 7 and 8). It was observed that *akt*, *enos*, and *irs-1* gene expressions in the ovarian tissues of the F group were significantly decreased when compared to the C group ($p < 0.05$), similar to Western Blot results. It was determined that these gene expressions, which decreased with fructose administration, increased with metformin administration alone (M group) ($p < 0.05$). The *enos* gene expression in the ovarian tissues of
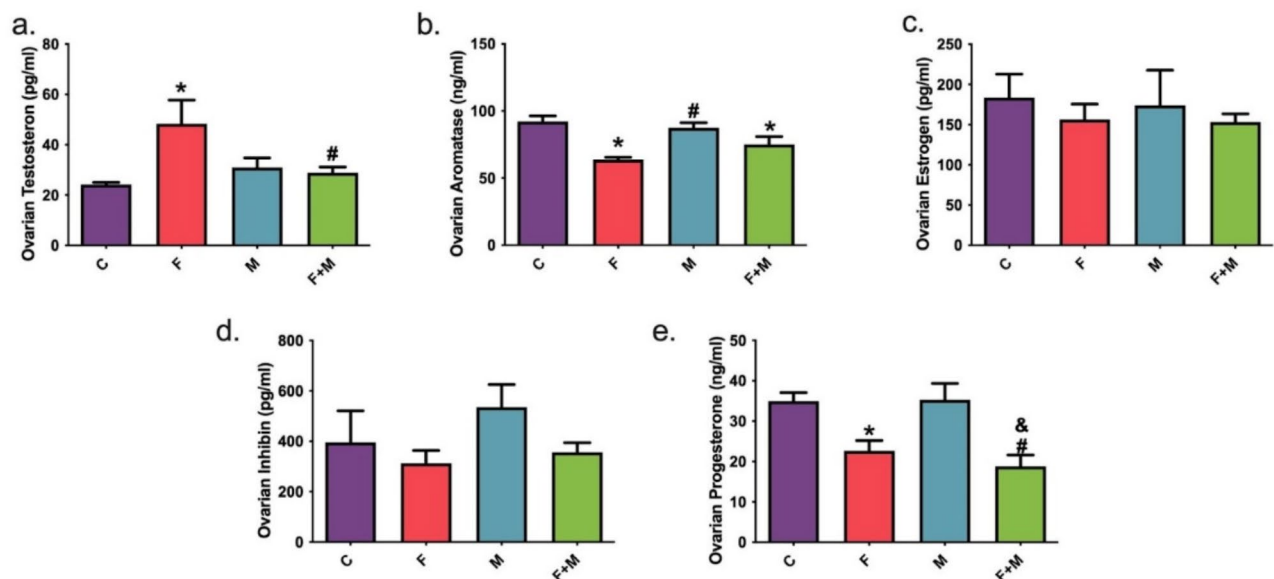
Fig. 5. The levels of (**a**) testosterone, (**b**) aromatase, (**c**) estrogen, (**d**) inhibin, and (**e**) progesterone in ovarian tissue. Each bar represents at least six rats. C: Control; F: Fructose; M: Metformin; F + M: Fructose + Metformin. *$p < 0.05$, significantly different from C group; # $p < 0.05$, significantly different from F group; &$p < 0.05$, significantly different from M group.

the F + M group increased significantly compared to the F group ($p < 0.05$). However, there was no significant difference in mRNA expression levels of *akt* and *irs-1* between the F and F + M groups.

The gene expressions of *mapk* and *bax* in the ovarian tissues of the F group were significantly increased compared to other groups ($p < 0.05$). The gene expressions of *jnk* and *bcl-2* were significantly decreased in the F group ($p < 0.05$) compared to other groups. However, metformin administration alone (M group) significantly decreased the gene expressions of *mapk*, *bax*, and *caspase-3* and increased gene expressions of *jnk* and *bcl-2* compared to the F group ($p < 0.05$). In the F + M group, *mapk*, *erk1/2*, and *bax* gene expression in ovarian tissues significantly decreased and increased *bcl-2* significantly compared to the F group ($p < 0.05$).

Histopathology of ovarian, oviduct, and uterine tissues

The histopathological views of ovarian, oviduct, and uterine tissues are presented in Fig. 9.

The number of primordial, secondary, and tertiary follicles is presented in Table 2. Generally, it was seen that fructose administration decreased the number of follicles and metformin treatment increased the number of follicles in high fructose-related metabolic syndrome. The number of secondary follicles decreased significantly in the F group compared to the M groups ($p < 0.05$). The tertiary follicles number also decreased in the F group and it was statistically different compared to the C group ($p < 0.05$). While multiple ovarian cysts were detected in the F group, the number of cysts decreased in the F + M group. The ovarian cyst was not seen in other groups.

No pathology was found in the epithelium and stroma of the oviducts in the C and M groups. In the F group, edema and hydropic degeneration in the oviduct epithelium of 4 rats, and mild edema in the oviduct stroma of 2 rats were observed. Hydropic degeneration of the oviduct epithelium of one rat and mild edema in the oviductal stroma of one rat were detected in the F + M group.

While there were mild signs of inflammation in the uterine tissues of some rats in the F + M group, severe inflammation was detected in the uterine tissue of all rats in the F group. Mild epithelial proliferation was observed in the uterine endometrial glands of the group (F + M group), except for the C, F, and M groups. In the F group, epithelial proliferation ($n = 8$), cystic dilatation ($n = 1$), epithelial inflammatory cell infiltration ($n = 4$), apoptosis ($n = 1$), and squamous metaplasia ($n = 1$) were noted. Uterine stroma was found to be normal in the C and M groups. Congestion was detected in the vessels of the uterine stroma of all rats in the F group. In only one rat in the F + M group, congestion was detected in the vessels of the uterine stroma.

The estrogen, progesterone, and testosterone receptors level in reproductive tissues

The immunohistochemical expressions of estrogen, progesterone, and testosterone receptors in the endometrium, ovarian, and oviduct tissues are given in Fig. 10. There was no difference among the groups in estrogen, progesterone, and testosterone receptors in the *uterine gland epithelium* ($p > 0.05$). However, it was observed that progesterone and testosterone receptors increased in the fructose-administered groups compared to the C group. Additionally, these receptors were decreased in the F + M group compared to the F group. Progesterone receptors in the *uterine stroma* increased in the F group and decreased with metformin treatment (F + M). It was noted that testosterone receptors increased in the F group compared to the other groups. However, there was no difference among the groups in estrogen, progesterone, and testosterone receptors in the uterine
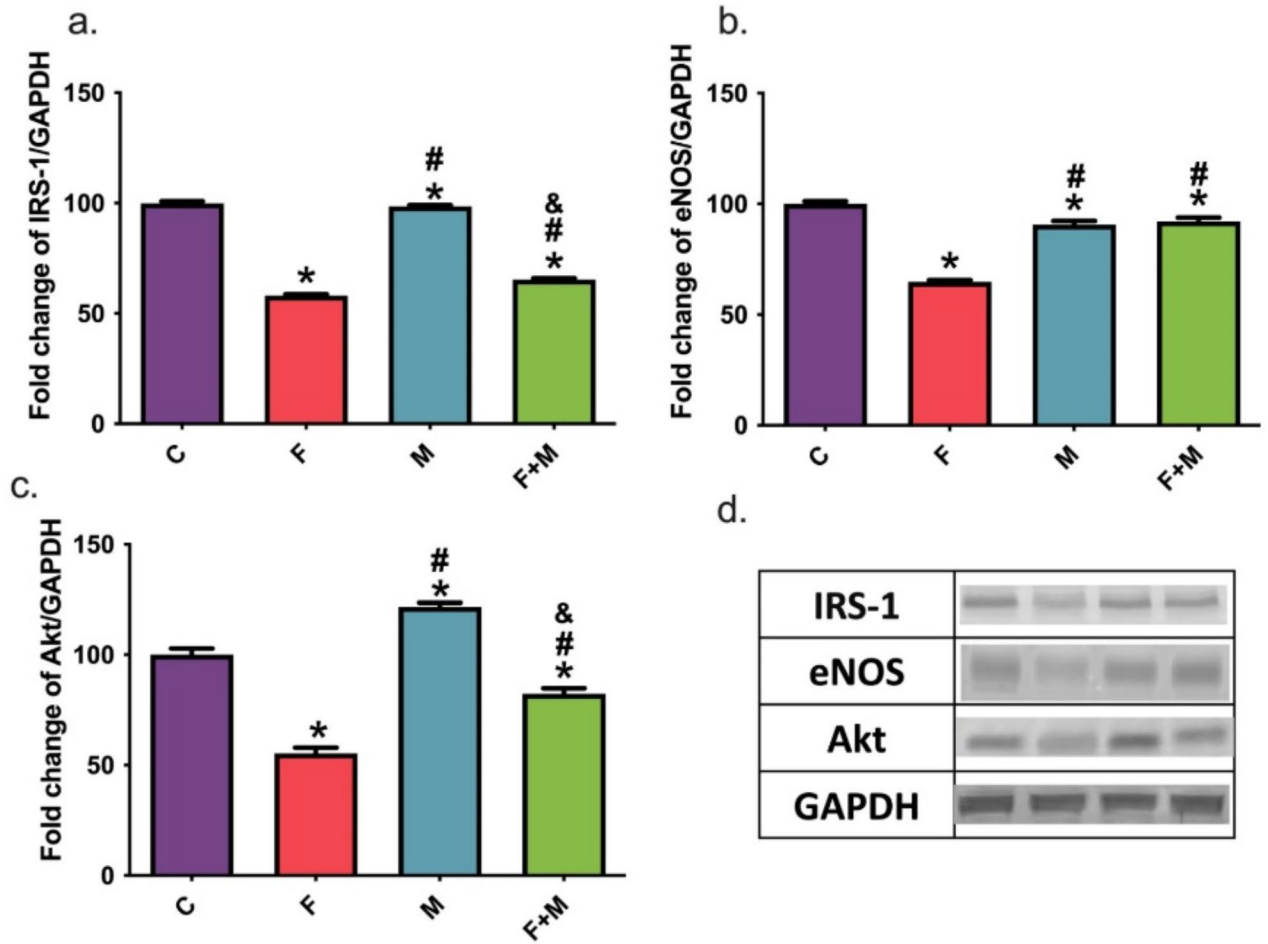
Fig. 6. The protein expression levels of (**a**) insulin receptor substrate (IRS-1), (**b**) endothelial nitric oxide synthase (eNOS), (**c**) protein kinase B (Akt), (**d**) representative Western blot images of proteins. Each bar represents at least six rats. C: Control; F: Fructose; M: Metformin; F + M: Fructose + Metformin. *$p < 0.05$, significantly different from C group; # $p < 0.05$, significantly different from F group; &$p < 0.05$, significantly different from M group.
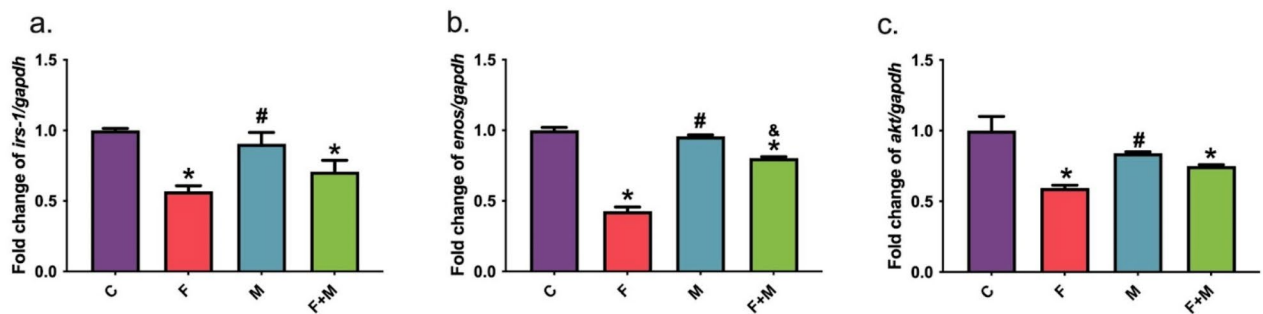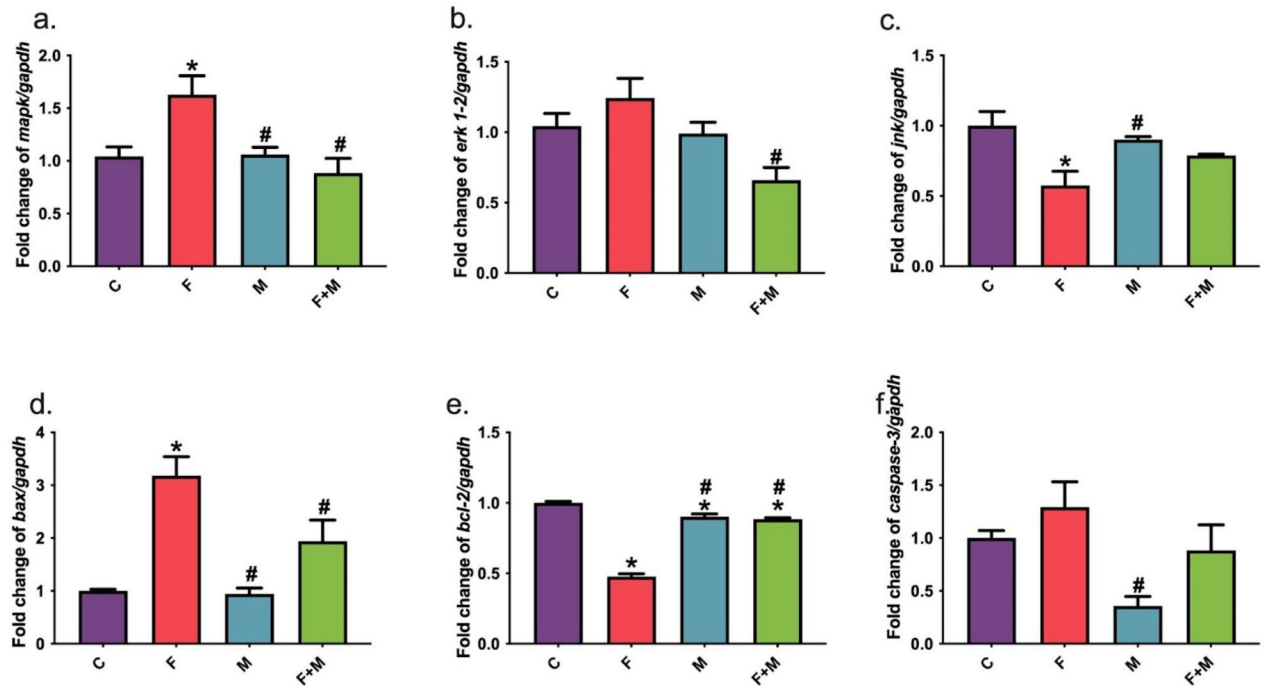

Fig. 7. The mRNA expression levels of (**a**) irs-1, (**b**) enos, (**c**) akt. Each bar represents at least six rats. C: Control; F: Fructose; M: Metformin; F + M: Fructose + Metformin. *$p < 0.05$, significantly different from C group; # $p < 0.05$, significantly different from F group; &$p < 0.05$, significantly different from M group.

Fig. 8. The mRNA expression levels of (**a**) mapk, (**b**) erk 1–2, (**c**) jnk, (**d**) bax, (**e**) bcl-2, (**f**) caspase-3. Each bar represents at least six rats. C: Control; F: Fructose; M: Metformin; F + M: Fructose + Metformin. *$p < 0.05$, significantly different from C group; # $p < 0.05$, significantly different from F group; &$p < 0.05$, significantly different from M group.

stroma ($p > 0.05$). No progesterone receptor was found in the *ovarian follicles* and *stroma* in all groups. Follicle testosterone receptor was seen in three rat's ovarian tissues in the F group and one rat's ovarian tissue in the F + M group. Testosterone receptor in the stroma was detected in two rats' ovarian tissues in the F group and one rat's ovarian tissue in the F + M group. There was no difference among the groups in estrogen, progesterone, and testosterone receptors in the ovarian follicle and stroma ($p > 0.05$). Estrogen and testosterone receptors were not found in all groups' *glandular epithelium* and *stroma of the oviduct*. Progesterone receptors in the glandular epithelium and stroma of the oviduct were decreased in the F group compared to other groups. It was observed that progesterone receptors increased with metformin treatment (M and F + M groups). However, there was no difference between the groups ($p > 0.05$) in estrogen, progesterone, and testosterone receptors in the oviduct gland epithelium and stroma.

Vaginal microbiota profile

Table 3 presents the Shannon and Chao1 alpha-diversity indices for the samples, indicating no significant difference between the groups. Principal components (PCs) were calculated using the ClustVis web tool, and corresponding PC values were visualized as scatterplots within JMP Pro 13. Microbiota composition analysis revealed distinct clustering for the F + M samples,, while the other samples did not display any clear clustering pattern (Fig. 11). In Fig. 12, the relative abundances of the ten most common phyla were plotted for each group. Proteobacteria, Firmicutes, and Bacteroidetes accounted for approximately 80% of the total phyla in all samples. Notably, Fusobacteria were more prevalent, and Firmicutes were less prevalent in the metformin-only group compared to the other treatment groups. In Figs. 13, 14, 15 and 16 the relative abundances of the twenty most common genera were plotted for each group. *Proteus* spp., *Aggregatibacter* spp., Gemellaceae, Enterobacteriaceae, *Morganella* spp., and *Streptococcus* spp. were the most prevalent genera for all groups. Besides that, the relative abundance of *Fusobacterium* spp. were more abundant in the metformin-only group than in the control group.

The response screening analysis yielded a comprehensive evaluation of genus-level differences across the groups. No statistically significant differences were observed between the F and C groups, or between the M and F + M groups. However, the C group exhibited a higher relative abundance of *Vibrio* and *Actinomyces* species compared to the M group, although this difference approached but did not reach statistical significance ($p = 0.05$). Additionally, *Vibrio* spp. exhibited a significantly higher relative abundance in the F group compared to the M group ($p < 0.05$). The F + M group had a notably greater prevalence of *Allobaculum* spp., Lachnospiraceae, *Oscillospira* spp. ($p < 0.05$), and Ruminococcaceae ($p < 0.01$) in comparison to the C group. Additionally, compared to the F group, the F + M group showed a significantly lower abundance of Ruminococcaceae ($p < 0.01$) and a significantly higher abundance of Oscillospira spp., Lachnospiraceae, and Christensenellaceae ($p < 0.05$).
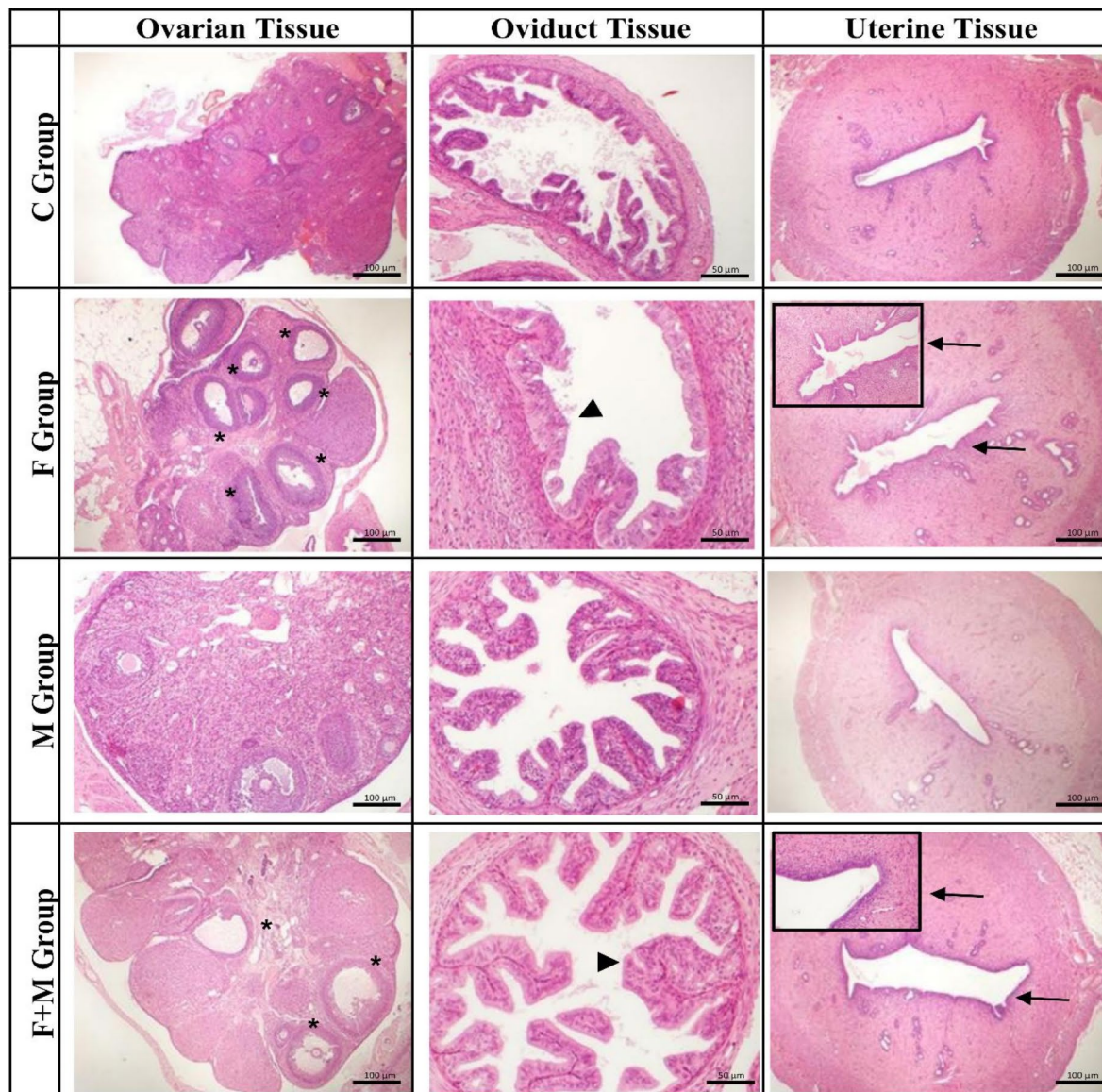
Fig. 9. Histopathological images from ovarian, oviduct, and uterine tissues in all groups. C Group: Normal appearance of ovarian, oviduct, and uterine tissues; F Group: Multiple ovarian cysts (star), severe hydropic degeneration and edema in the oviduct (arrowhead), epithelial inflammatory cell infiltration in the uterine tissue (arrow); M Group: Normal appearance of ovarian, oviduct, and uterine tissues; F + M Group: Ovarian cysts (star), hydropic degeneration and edema in the oviduct (arrowhead), cell infiltration in the uterine tissue (arrow); C: Control; F: Fructose; M: Metformin; F + M: Fructose + Metformin. Ovarian tissue HE100 µm; Oviduct tissue HE50 µm, Uterine tissue HE100 µm.

Discussion

Metabolic diseases, including metabolic syndrome, obesity, and type 2 diabetes, can affect female fertility and cause infertility. Previous studies revealed that metabolic syndrome, caused by high fructose in the diet, can also have a negative impact on female fertility[40–42,56–58]. In the present study, we investigated the effects of a high fructose diet on reproductive tissue and vaginal microbiota, and the therapeutic value of metformin administration in rats. Our results showed that a high fructose diet increased the serum glucose, insulin, and triglyceride levels. However, the elevation of testosterone levels and a reduction of aromatase levels in ovarian tissues were observed with the high fructose diet model. Moreover, a high fructose diet impaired the insulin signaling pathway proteins including Akt, eNOS, and IRS1 in the ovarian tissue. Furthermore, there was a decrease in mRNA expression levels of *act-1*, *enos*, *irs-1*, *jnk*, and *bcl-2* but an increase in *mapk* and *bax* genes in ovarian tissue of high fructose-fed rats. It was also determined that a high fructose diet might decrease the number of ovarian follicles, and lead to the development of ovarian cysts, and cause oviduct and uterine

	C Group	F Group	M Group	F + M Group
Primordial follicles	4.00 ± 2.40	2.40 ± 0.73	4.70 ± 0.76	4.30 ± 0.37
Secondary follicles	3.70 ± 0.71	2.10 ± 0.52	4.30 ± 0.49#	3.00 ± 0.27
Tertiary follicles	4.50 ± 1.00	1.40 ± 0.32*	2.00 ± 0.45	2.10 ± 0.30

Table 2. The comparison according to groups of the primordial, secondary, and tertiary follicle numbers. Values are expressed as mean ± SEM. C: Control; F: Fructose; M: Metformin; F + M: Fructose + Metformin. *$p < 0.05$, significantly different from C group; # $p < 0.05$, significantly different from F group, $n = 6$–8.
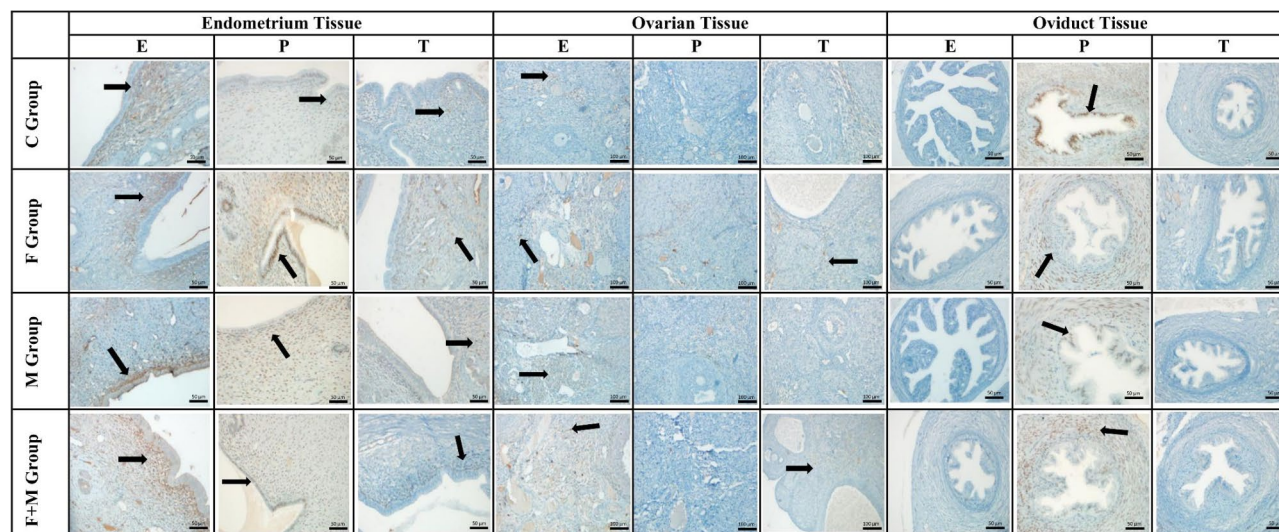

Fig. 10. Immunohistochemical analysis of estrogen, progesterone, and testosterone receptors (arrow) of endometrium, ovarian, and oviduct tissues in all groups. C: Control; F: Fructose; M: Metformin; F + M: Fructose + Metformin. Endometrium tissue immunohistochemistry 50 μm; Ovarian tissue immunohistochemistry 100 μm; Oviduct tissue immunohistochemistry 50 μm.

Chao1			
	C	F	M
F	0.64	–	–
M	1.00	0.64	–
F + M	0.29	0.31	0.29
Diversity_shannon			
	C	F	M
F	0.74	–	–
M	0.74	0.74	–
F + M	0.36	0.74	0.74

Table 3. p-values derived from Shannon and Chao1 alpha-diversity indexes of the samples.

pathologies. The number and diversity of bacteria in the vaginal microbiota altered with a high fructose diet in rats. The results of the present study indicated that metformin treatment modulated these parameters in high fructose diet-induced metabolic syndrome in rats. The degeneration caused by high fructose in the rat ovary may be induced by the disruption of proteins in the insulin signaling system and the activation of apoptotic pathways. The curative effect of metformin on these pathways in the serum and ovarian tissue, and the vaginal microbiota profile may have a direct connection with improving infertility caused by a high fructose diet.

Fructose is a fruit sugar commonly used as a flavor enhancer in foods. Fructose, an intermediate molecule of glucose metabolism, is rapidly absorbed and metabolized by the liver. A high fructose diet stimulates lipogenesis, leading to triglyceride and cholesterol accumulation in the liver. Subsequently, the sensitivity of insulin is reduced, and insulin resistance and glucose intolerance develop. Several studies have shown that administration of the high-fructose diet in rats causes MetS with hyperglycemia, hyperinsulinemia, insulin resistance, dyslipidemia,
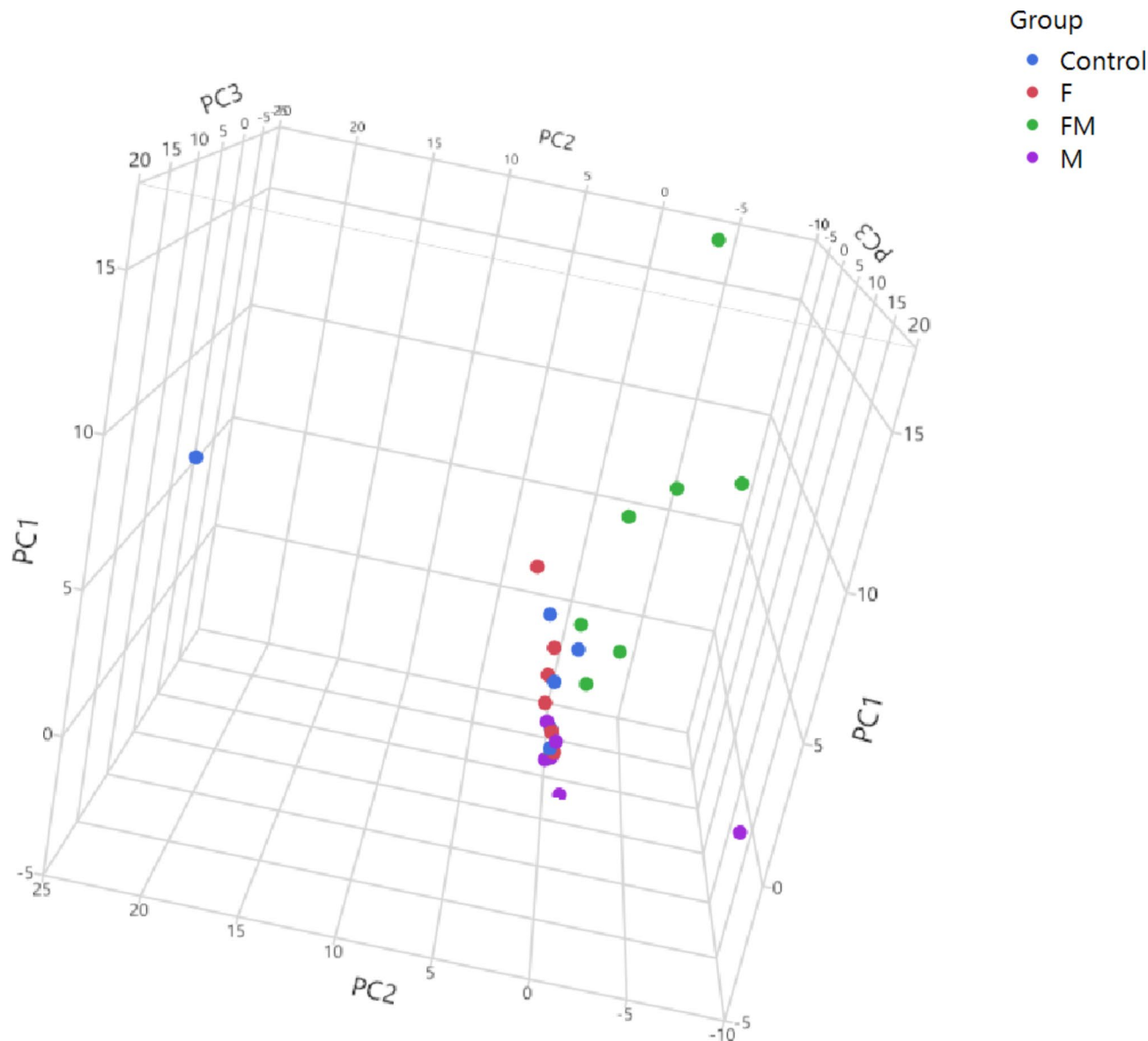
Fig. 11. A scatterplot of the first 2 PCs was calculated for the microbiota composition of the samples.

weight gain, and hypertension[59–63]. In a study conducted on male and female rats on a high fructose diet, it was stated that the increase in blood glucose, insulin, and lipid profile was similar in both genders[64]. Metformin (dimethylbiguanide), a first-line oral blood glucose-lowering agent to control type 2 diabetes mellitus, has been used because of its safety, low cost, and effectiveness in improving hyperglycemia with $\geq 1.5\%$ HbA1c reduction for many years. Metformin decreases blood glucose levels and improves insulin sensitivity by reducing hepatic glucose production, increasing glucose utilization by skeletal muscle, and regulating lipid metabolism. Therefore, it has been known that metformin is used to reduce metabolic syndrome risk factors[59,65–68]. In the present study, the serum glucose and triglyceride levels exhibited a higher concentration in the F group when compared to that of the other groups in female rats. Insulin levels in the F group were elevated than in the C group ($p < 0.05$). However, total cholesterol, LDL, and HDL levels showed no change among the groups. Metformin treatment was found to lower serum glucose, triglycerides, and insulin levels. Similar to other studies, our results also provide evidence that a high fructose diet increased serum glucose, and triglyceride levels, and metformin treatment was effective in improving these parameters. The findings confirmed that metformin could be used as a treatment option with its anti-diabetic and anti-lipidemic activity in high-fructose diet-induced metabolic syndrome.

Many studies indicate that aromatase activity can be disturbed due to insulin resistance and metabolic syndrome in females. Therefore, elevated androgen levels and decreased estrogen and progesterone levels can mainly be observed in metabolic syndrome. As a result, it has been revealed that impaired folliculogenesis, anovulation, and spontaneous miscarriages may occur in females with metabolic syndrome[41,69,70]. Although metformin is known to have beneficial effects on ovarian physiology, its exact mechanisms of action are still unclear. Previous studies demonstrated that metformin has therapeutic effects on follicular development and
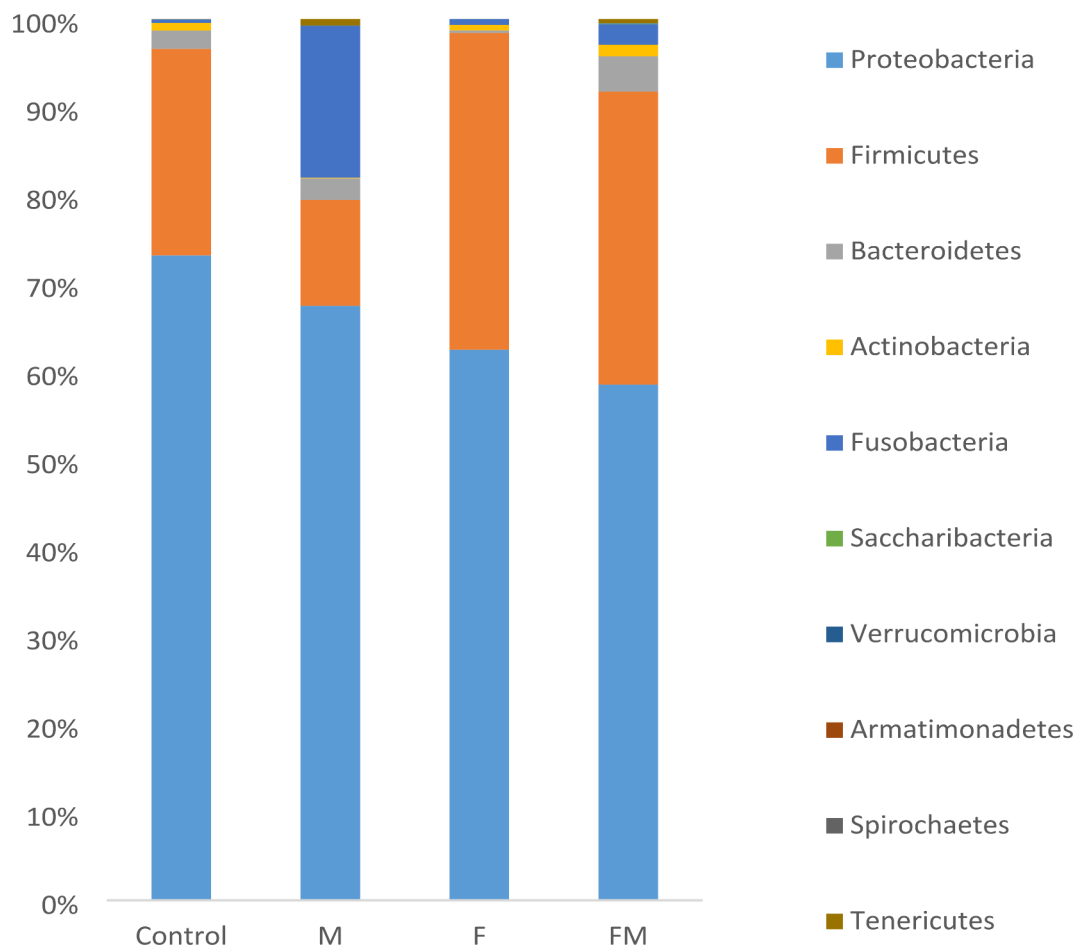
Fig. 12. Relative abundances of the ten most prevalent bacterial phyla in all treatment groups.

ovarian angiogenesis[31,32,71]. Additionally, there are opinions that metformin regulates aromatase activity[33,72,73]. In the current study, serum aromatase, inhibin, estrogen, progesterone, and testosterone levels showed no change among the groups. Although there was no statistical difference in the F group compared to other groups, it was noticed that serum testosterone levels increased with a high-fructose diet. Metformin treatment (M and F + M groups) was found to lower serum testosterone levels. Similar to other studies, our results also provide evidence that high fructose diet increased serum testosterone levels and decreased aromatase levels, and metformin treatment was effective in improving these parameters. Ovarian tissue estrogen and inhibin levels were not different among all groups. Although the tissue progesterone levels in the F and M groups were similar to that of the C group, it was different compared to the F + M group. Ovarian tissue testosterone levels were markedly increased in the F group when compared to those of other groups. Tissue testosterone levels in rats treated with metformin in combination with a high fructose diet were significantly lower than in rats given a high fructose diet al.one. A high fructose diet was found to reduce tissue aromatase levels. The tissue aromatase level in the M group was similar to that of the C group. There was a significant tissue aromatase level differential between the M group and the F + M group. It was thought that these changes in steroid hormones might vary according to the estrus cycle stage. However, it was observed a high fructose diet increased testosterone levels by disrupting tissue aromatase activity. It is suggested that metformin treatment can positively affect fertility by improving aromatase activity. As a result, it was considered that metformin administration is effective in the regulation of steroid hormones in rats with MetS.

Insulin exerts its cellular effect by binding to specific receptors and mediating signal amplification cascades through insulin receptor substrates[74]. In addition, insulin may interfere with the mitogenesis-related mapk/erk1-2 and the apoptosis-related JNK-Bcl2-Bax pathway via regulation of AKT phosphorylation[75,76].

Insulin signaling has a variety of roles in ovarian function, including controlling steroidogenesis, follicular growth, and granulosa cell proliferation, although the ovary is not a typical target tissue for insulin[77]. Moreover, several studies suggest that female mice lacking essential insulin signaling pathway components, such as IRS2, may be infertile and lack ovarian and hypothalamic function[78,79]. Studies have shown that high-calorie diets disrupt ovarian insulin signaling and cause ovarian dysfunction in female rats. It was reported that ovarian IRS1, IRS2, PI3K expression, and AKT phosphorylation were decreased with a high-fat diet for 180 days in female rats[80]. Liu et al. reported that the co-administration of letrozole and a high-fat diet in rats resulted in the suppression of the ovarian PI3K/AKT/mTOR pathway and upregulation of proteins involved in autophagy
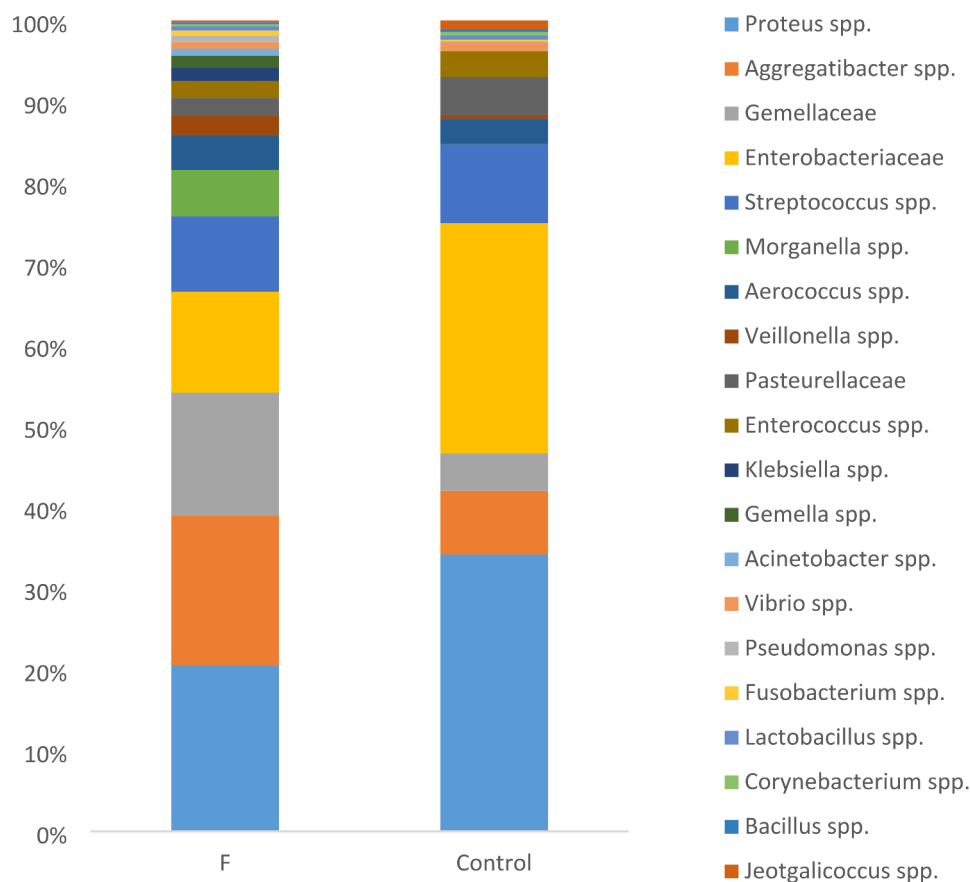
Fig. 13. Relative abundances of the twenty most prevalent bacterial genera in the F group compared to the C group.

and apoptosis such as cleaved-caspase 3,9 and beclin[81]. Hyperinsulinemia, a key indicator of insulin resistance, is reported to be associated with ovarian hyperandrogenism by stimulating ovarian stromal androstenedione and testosterone synthesis[82,83]. As an insulin sensitizer, metformin is used in the treatment of PCOS, the main symptoms of which are hyperinsulinemia and hyperandrogenemia[84,85]. Experimental studies with high-fat diet and PCOS-inducing agents have indicated that metformin suppresses ovarian AKT/mTOR/autophagy signaling pathways and also reduces excessive autophagy in ovarian granulosa cells through the PI3K/AKT/mTOR pathway[32,86]. Although several studies have reported that high-fructose diets affect ovarian tissue and hormone balance, to our knowledge, no study has examined ovarian insulin signaling and apoptosis pathways in high-fructose-fed rats. Therefore, we investigated the interference of a high fructose diet on the mitogenic MAPK pathway or apoptosis mediated by IRS-1/AKT and eNOS and the possible therapeutic effect of metformin.

In this study, the expression of akt-1, enos, and irs-1 genes was significantly decreased in the ovarian tissues of the F group. In contrast, these parameters were significantly increased in the high fructose and metformin-treated group (F + M group). These findings were also confirmed by our western blot results. The results showed that metformin treatment may have beneficial effects on high fructose diet-induced disrupted ovarian insulin signaling pathway. In addition, we revealed that ovarian mapk, apoptotic jnk, and bax gene expressions were increased in the high fructose group. In contrast, bcl-2 gene expression decreased when the ovarian tissues of the F group were compared with the other groups. On the other hand, the group receiving metformin treatment with fructose (F + M group), mapk, erk1/2, and bax gene expressions were markedly decreased, and bcl-2 gene expression was significantly increased compared to the F group. Considering these findings, it has been shown that metformin treatment has an ameliorative effect on insulin and mapk signaling pathways and apoptotic-related gene expressions in high fructose diet-induced metabolic syndrome in rats.

The observation of histopathological changes in the ovarian, oviduct, and uterine tissues also contributes to the determination of the pathogenesis of the reproductive system disease[87]. It has been known that MetS may lead to polycystic ovary syndrome, ovulation dysfunction, and hyperandrogenism[88,89]. In a previous study, it was observed rats fed a high fructose diet (55%) had squamous metaplasia in the uterine tissue and congestion in the ovarian tissue[90]. In the current study, it was determined that a high fructose diet could cause pathologies in the ovarian, oviduct, and uterine tissues. While a high fructose diet decreased the number of ovarian follicles and stimulated cyst development, metformin treatment increased the number of follicles and reduced the number of cysts. However, edema and hydropic degeneration in the oviduct, inflammation, epithelial proliferation, cystic
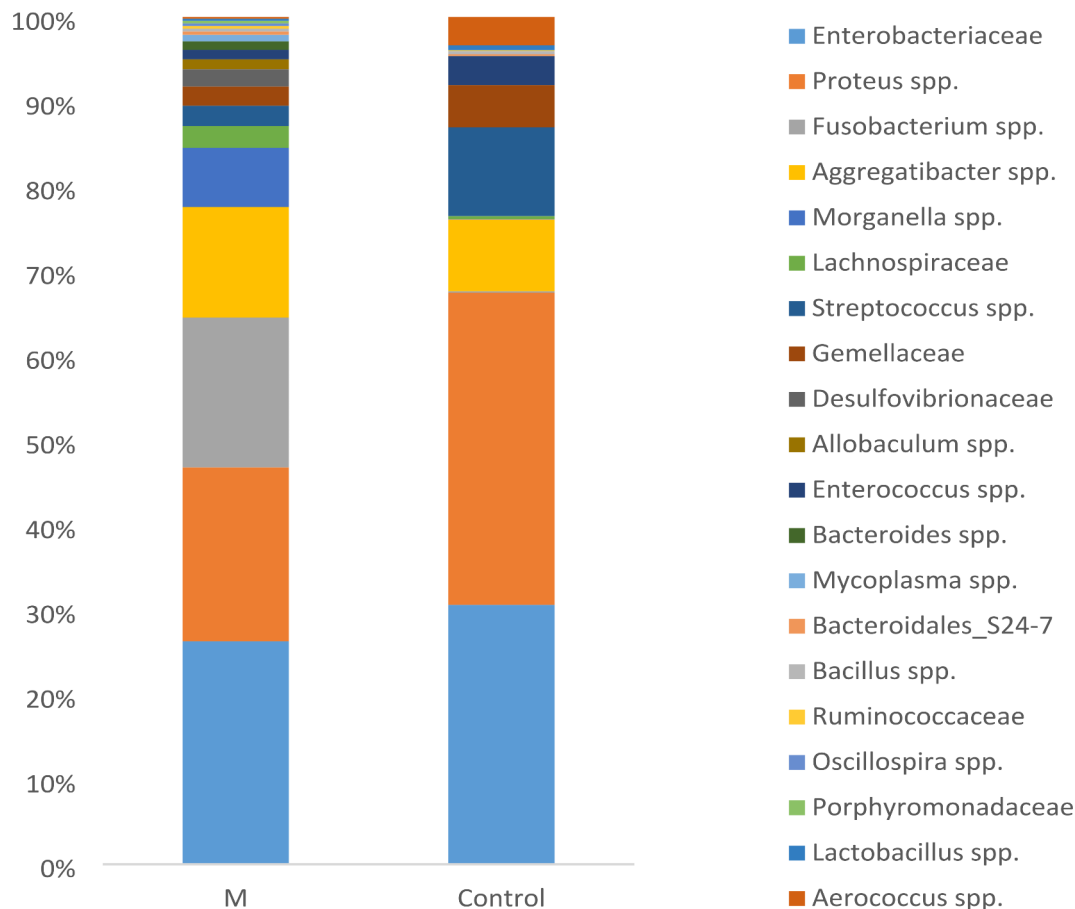
Fig. 14. Relative abundances of the twenty most prevalent bacterial genera in the M group compared to the C group.

dilatation, and squamous metaplasia in the uterine tissue were seen in rats fed a high fructose diet. Although there was no difference among groups in estrogen, progesterone, and testosterone receptor levels in the ovarian, oviduct, and uterine tissues, fructose administration generally caused an increase in testosterone receptors in the ovarian and uterine tissues. The increase in the number of testosterone receptors in the follicles and the occurrence of follicular cysts in rats fed a high-fructose diet compared to the other groups suggested that it may cause infertility in females. However, metformin treatment can provide a modulation in these receptors. These results were also consistent with blood hormone levels. According to these results, it was thought that a high fructose diet could negatively affect reproductive tissues and may cause infertility in the future, and metformin may contribute to the treatment. It was suggested that the histopathological changes of the reproductive tissues could be improved by metformin administration in cases with metabolic syndrome.

The vaginal microbiota plays a pivotal role in female well-being and reproductive outcomes[91]. *Lactobacillus* species are the predominant bacteria in the vaginal environment and contribute to preserving a healthy vaginal environment[92]. The vaginal microbial community is characterized by the prevalence of *Lactobacillus* while also encompassing other aerobic and anaerobic species. Perturbation of the vaginal ecosystem can result in the proliferation of pathogens and the emergence of vaginal infections[93]. *Lactobacillus* spp. have been extensively employed as a preventative and therapeutic intervention against vaginal pathogens[94]. However, the comprehension of the linkage between the vaginal microbiota and vaginal well-being remains restrained. Further examinations are needed to acquire a more thorough comprehension of the complexities of the vaginal microbiota and its function in supporting vaginal and reproductive health. Therefore, we investigated the changes in vaginal microbiota caused by a high fructose diet and the effect of metformin.

In the present study, the F group exhibited a significantly larger abundance of *Vibrio* spp. in comparison to the M group. *Vibrio* spp. is known to be associated with various infections[95], such as vibriosis causing abortion[96], cholera[97], and gastroenteritis[98,99]. Additionally, *Actinomyces* spp., which were found in greater abundance in the C group compared to the M group, are recognized as opportunistic pathogens linked to actinomycosis, a chronic disease characterized by the formation of abscesses, primarily affecting the oral cavity and other mucosal surfaces[100–102]. These findings suggest that the M group (M) may harbor fewer potential pathogens compared to the F and C groups, as evidenced by the lower abundance of *Vibrio* and *Actinomyces* spp. Furthermore, no significant differences were observed between the M and F+M groups, indicating that the combination of treatments did not lead to increased pathogenic bacterial presence.
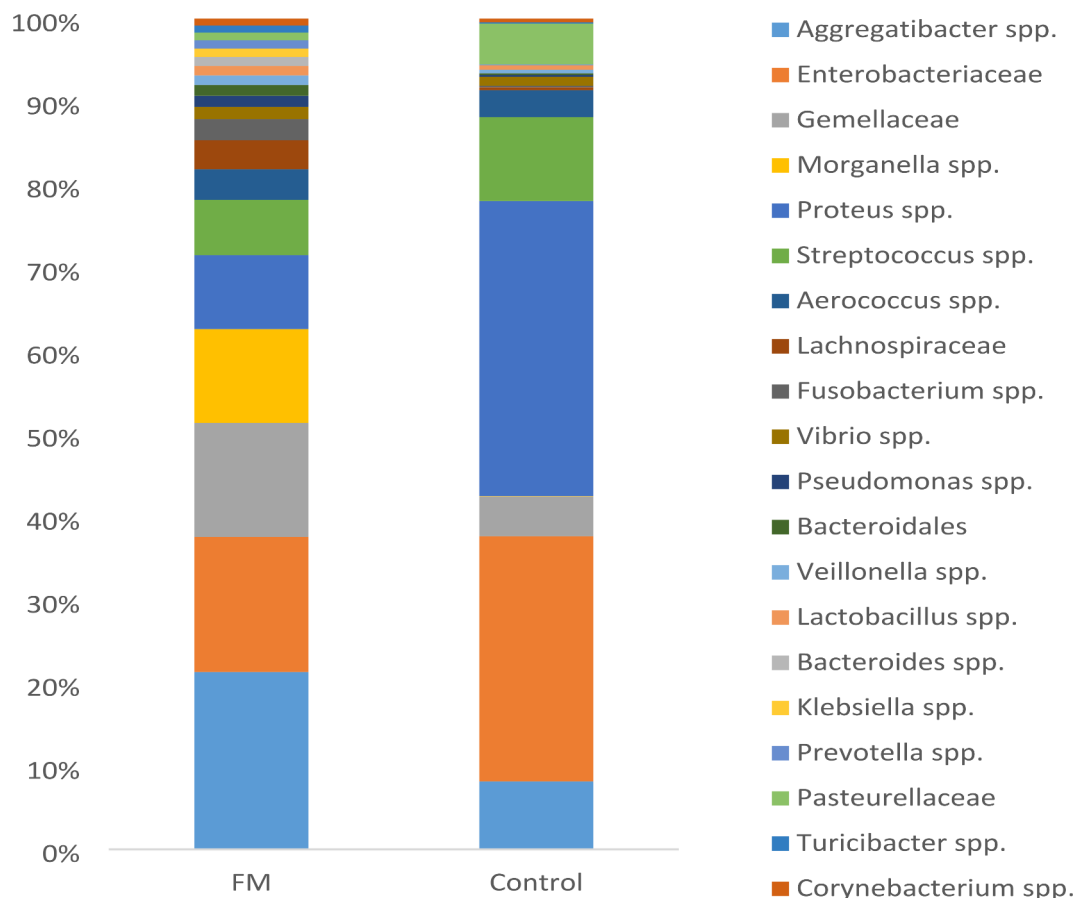
Fig. 15. Relative abundances of the twenty most prevalent bacterial genera in the FM group compared to the C group.

Compared to the C group, the F + M group exhibited a higher abundance of *Allobaculum* spp., *Oscillospira* spp., Lachnospiraceae, and Ruminococcaceae, associated with beneficial and protective effects[103–108]. Additionally, the F + M group exhibited a higher prevalence of *Oscillospira* spp., Lachnospiraceae, and Christensenellaceae than the F group. However, the F group had a higher abundance of Ruminococcaceae, possibly influenced by infectious members within this bacterial family. Oscillospira spp., in particular, has been negatively correlated with obesity and is considered a marker of metabolic health[109]. Similarly, members of the Christensenellaceae family have also been associated with gut health and negatively correlated with obesity and metabolic syndrome[110–113]. The increased prevalence of these bacteria indicated that metformin may induce the proliferation of probiotic bacteria in vaginal microbiota.

Conclusion

In conclusion, our results highlight the deleterious effects of a high fructose diet on the metabolic and reproductive systems as well as the vaginal microbiota in female rats. A high fructose diet causes increased blood glucose, triglyceride, insulin, and ovarian testosterone levels, as well as decreased ovarian aromatase levels, reduced follicle number, and uterine inflammation. These effects are thought to result from the down-regulation of ovarian insulin signaling pathway proteins (Akt, IRS-1 and e-NOS) and dysregulation of mitogenic (increased Mapk and decreased jnk expression levels) and apoptotic (increased bax and decreased bcl-2 expression levels) pathway proteins. Moreover, it has been predicted that a high-fructose diet may lead to dysbiosis in the vaginal microbiota. Our findings suggest that metformin may improve ovarian disorders through hormonal balance, modulation of Mapk and apoptotic signaling molecules, and regulation of vaginal microbiota. To our knowledge, our study is the first to demonstrate the effects of metformin on ovarian molecular mechanisms and vaginal microbiota in the context of a high fructose diet. Our research further extends the understanding of metformin's regulatory effects on the vaginal microbiota. The experimental evidence suggests that metformin has a broader systemic impact. Furthermore, we measured key parameters in the identified molecular pathways, but not all parameters were assessed and transcriptional differences in other parameters were not investigated. Finally, the effects of high fructose and metformin on fertility in animals have not been established. Therefore, further research is needed to more accurately define the molecular mechanisms underlying the protective and therapeutic effects of metformin in high fructose diet-induced female infertility.
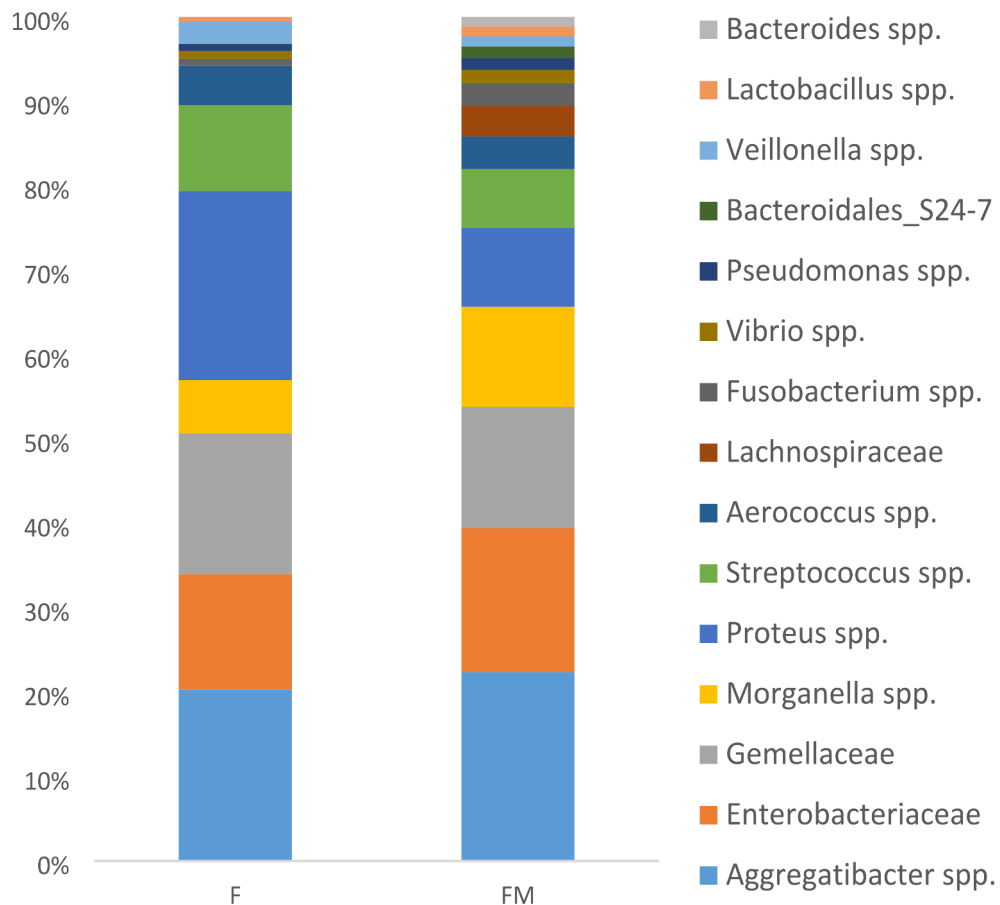
Fig. 16. Relative abundances of the twenty most prevalent bacterial genera in the F group compared to the F + M group.

References
1. Fahed, G. et al. Metabolic syndrome: updates on pathophysiology and management in 2021. *Int. J. Mol. Sci.* **23**, 786 (2022).
2. Hayden, M. R. Overview and New insights into the metabolic syndrome: risk factors and emerging variables in the development of type 2 diabetes and Cerebrocardiovascular Disease. *Med. (Lithuania)* **59**, 561 (2023).
3. Akar, F., Sumlu, E., Alçığır, M. E., Bostancı, A. & Sadi, G. Potential mechanistic pathways underlying intestinal and hepatic effects of kefir in high-fructose-fed rats. *Food Res. Int.* **143**, 110287 (2021).
4. Sumlu, E., Bostancı, A., Sadi, G., Alçığır, M. E. & Akar, F. Lactobacillus plantarum improves lipogenesis and IRS-1/AKT/eNOS signalling pathway in the liver of high-fructose-fed rats. *Arch. Physiol. Biochem.* **128**, 786–794 (2022).
5. Lubawy, M. & Formanowicz, D. High-fructose Diet-Induced Hyperuricemia accompanying metabolic syndrome-mechanisms and dietary therapy proposals. *Int. J. Environ. Res. Public Health* **20**, 3596 (2023).
6. Martins, A. D., Majzoub, A. & Agawal, A. Metabolic syndrome and male fertility. *World J. Men's Health* **37**, 113–127 (2019).
7. Cohen, D. J. et al. Metabolic syndrome and male fertility disorders: is there a causal link? *Reviews Endocr. Metabolic Disorders* **22**, 1057–1071 (2021).
8. Marchiani, S., Tamburrino, L., McPherson, N. & Baldi, E. The role of obesity and metabolic syndrome in couple infertility. *Front. Endocrinol.* **12**, 784716 (2021).
9. Salvio, G. et al. Metabolic syndrome and male fertility: Beyond Heart consequences of a Complex Cardiometabolic Endocrinopathy. *Int. J. Mol. Sci.* **23**, 5497 (2022).
10. Guney, C., Bal, N. B. & Akar, F. The impact of dietary fructose on gut permeability, microbiota, abdominal adiposity, insulin signaling and reproductive function. *Heliyon* **9**, e18896 (2023).
11. Al Awlaqi, A., Alkhayat, K. & Hammadeh, M. E. Metabolic syndrome and infertility in women. *Int. J. Women's Health Reprod. Sci.* **4**, 89–95 (2016).
12. He, Y. et al. Influence of metabolic syndrome on female fertility and in vitro fertilization outcomes in PCOS women. *Am. J. Obstet. Gynecol.* **221**, 138e1–138e12 (2019).

13. Cena, H., Chiovato, L. & Nappi, R. E. Obesity polycystic ovary syndrome, and infertility: a New Avenue for GLP-1 receptor agonists. *J. Clin. Endocrinol. Metab.* **105**, e2695–e2709 (2020).
14. Westerman, R. & Kuhnt, A. K. Metabolic risk factors and fertility disorders: a narrative review of the female perspective. *Reprod. Biomed. Soc.* **14**, 66–74 (2022).
15. Akar, F. et al. Dietary high-fructose reduces barrier proteins and activates mitogenic signalling in the testis of a rat model: Regulatory effects of kefir supplementation. *Andrologia* **54**, 1–12 (2022).
16. Wang, M. X., Yin, Q. & Xu, X. A rat model of polycystic ovary syndrome with insulin Resistance Induced by Letrozole combined with high Fat Diet. *Med. Sci. Monitor: Int. Med. J. Exp. Clin. Res.* **26**, e922136 (2020).
17. Khan, D., Sridhar, A., Flatt, P. R. & Moffett, R. C. Disturbed ovarian morphology, oestrous cycling and fertility of high fat fed rats are linked to alterations of incretin receptor expression. *Reprod. Biol.* **23**, 100784 (2023).
18. Jayasinghe, I. U., Agampodi, T. C., Dissanayake, A. K., Srimantha, S. M. & Agampodi, S. B. Comparison of global definitions of metabolic syndrome in early pregnancy among the Rajarata Pregnancy Cohort participants in Sri Lanka. *Sci. Rep.* **2022**, 12 (2009).
19. Yang, Y. et al. Cardiac remodeling during pregnancy with metabolic syndrome: Prologue of pathological remodeling. *Circulation* **143**, 699–712 (2021).
20. Hou, K. et al. Microbiota in health and diseases. *Signal. Transduct. Target. Therapy* **7**, 135 (2022).
21. Krupa-Kotara, K., Helisz, P., Gwioździk, W. & Grajek, M. The importance of the Microbiota in Shaping women's Health—the current state of knowledge. *Appl. Microbiol.* **3**, 11–34 (2023).
22. Villemin, C. et al. The heightened importance of the microbiome in cancer immunotherapy. *Trends Immunol.* **44**, 44–59 (2023).
23. Holdcroft, A. M., Ireland, D. J. & Payne, M. S. The vaginal microbiome in health and disease-what role do common intimate hygiene practices play? *Microorganisms* **11**, 298 (2023).
24. Vitale, S. G. et al. The role of genital tract microbiome in fertility: a systematic review. *Int. J. Mol. Sci.* **23**, 180 (2021).
25. Lledo, B. et al. Identification of vaginal microbiome associated with IVF pregnancy. *Sci. Rep.* **12**, 6807 (2022).
26. Günther, V. et al. Vaginal microbiome in reproductive medicine. *Diagnostics* **12**, 1–17 (2022).
27. Barrientos-Durán, A., Fuentes-López, A., de Salazar, A., Plaza-Díaz, J. & García, F. Reviewing the composition of vaginal microbiota: inclusion of nutrition and probiotic factors in the maintenance of eubiosis. *Nutrients* **12**, 1–30 (2020).
28. Dall'Asta, M. et al. Pre-pregnancy diet and vaginal environment in caucasian pregnant women: an exploratory study. *Front. Mol. Biosci.* **8**, 1–9 (2021).
29. Faure, M. et al. Metformin in reproductive biology. *Front. Endocrinol.* **9**, 1–12 (2018).
30. Nayak, G. et al. Antidiabetic drug metformin affects the developmental competence of cleavage-stage embryos. *J. Assist. Reprod. Genet.* **37**, 1227–1238 (2020).
31. Shpakov, A. O. Improvement effect of metformin on female and male reproduction in endocrine pathologies and its mechanisms. *Pharmaceuticals* **14**, 1–45 (2021).
32. Di Pietro, M. et al. Metformin regulates ovarian angiogenesis and follicular development in a female polycystic ovary syndrome rat model. *Endocrinology* **156**, 1453–1463 (2015).
33. Mahamed, R. R. et al. Metformin improves ovarian follicle dynamics by reducing theca cell proliferation and CYP-17 expression in an androgenized rat model. *J. Ovarian Res.* **11**, 18 (2018).
34. Xing, C. et al. Metformin and exenatide upregulate hepatocyte nuclear factor-4α, sex hormone binding globulin levels and improve hepatic triglyceride deposition in polycystic ovary syndrome with insulin resistance rats. *J. Steroid Biochem. Mol. Biol.* **214**, 105992 (2021).
35. He, X. et al. Metformin inhibits MAPK signaling and rescues pancreatic aquaporin 7 expression to induce insulin secretion in type 2 diabetes mellitus. *J. Biol. Chem.* **297**, 101002 (2021).
36. Herman, R., Kravos, N. A., Jensterle, M., Janež, A. & Dolžan, V. Metformin and insulin resistance: a review of the underlying mechanisms behind changes in GLUT4-Mediated glucose transport. *Int. J. Mol. Sci.* **23**, 1264 (2022).
37. Ma, L. et al. Low glucose and metformin-induced apoptosis of human ovarian cancer cells is connected to ASK1 via mitochondrial and endoplasmic reticulum stress-associated pathways. *J. Exp. Clin. Cancer Res.* **38**, 77 (2019).
38. Li, B. et al. Metformin induces cell cycle arrest, apoptosis and autophagy through ROS/JNK signaling pathway in human osteosarcoma. *Int. J. Biol. Sci.* **16**, 74–84 (2020).
39. Szymczak-Pajor, I. et al. Metformin induces apoptosis in human pancreatic Cancer (PC) cells accompanied by changes in the levels of histone acetyltransferases (particularly, p300/CBP-Associated factor (PCAF) protein levels). *Pharmaceuticals* **16**, 115 (2023).
40. Saben, J. L. et al. Excess maternal fructose consumption increases fetal loss and impairs endometrial decidualization in mice. *Endocrinology* **157**, 956–968 (2016).
41. Munetsuna, E. et al. Maternal fructose intake disturbs ovarian estradiol synthesis in rats. *Life Sci.* **202**, 117–123 (2018).
42. Rejani, C. T., Navin, A. K., Mumthaz, T. M. V. & Bhuvarahamurthy, V. High fat-high fructose diet elicits hypogonadotropism culminating in autophagy-mediated defective differentiation of ovarian follicles. *Cells* **11**, 3447 (2022).
43. Yildirim, O. G. et al. High-fructose in drinking water initiates activation of inflammatory cytokines and testicular degeneration in rat. *Toxicol. Mech. Methods* **29**, 224–232 (2019).
44. Quaile, M. P. et al. Toxicity and toxicokinetics of metformin in rats. *Toxicol. Appl. Pharmcol.* **243**, 340–347 (2010).
45. Dimauro, I., Pearson, T., Caporossi, D. & Jackson, M. J. A simple protocol for the subcellular fractionation of skeletal muscle cells and tissue. *BMC Res. Notes* **5**, 513 (2012).
46. Lowry, O. H., Rosebrough, N. J., Farr, A. L. & Randall, R. J. Protein measurement with the Folin phenol reagent. *J. Biol. Chem.* **193**, 265–275 (1951).
47. Wei, A. et al. Ozone therapy ameliorates inflammation and endometrial injury in rats with pelvic inflammatory disease. *Biomed. Pharmacotherapy = Biomed. Pharmacotherapie* **107**, 1418–1425 (2018).
48. Ravn, V. et al. Reproducibility of subjective immunohistochemical estrogen- and progesterone receptor determination in human endometrium. *Pathol. Res. Pract.* **189**, 1015–1022 (1993).
49. Odetola, S. S., Ajani, M. A., Iyapo, O., Salami, A. A. & Okolo, C. A. Hormonal receptor expression in endometrial carcinoma: a retrospective immunohistochemical study in a Nigerian Tertiary Hospital. *J. West. Afr. Coll. Surg.* **10**, 1–4 (2020).
50. Zheng, W. et al. An accurate and efficient experimental approach for characterization of the complex oral microbiota. *Microbiome* **3**, 48 (2015).
51. Caporaso, J. G. et al. QIIME allows analysis of high-throughput community sequencing data. *Nat. Methods* **7**, 335–336 (2010).
52. Callahan, B. J. et al. DADA2: high-resolution sample inference from Illumina amplicon data. *Nat. Methods* **13**, 581–583 (2016).
53. Metsalu, T., Vilo, J. & ClustVis A web tool for visualizing clustering of multivariate data using principal component analysis and heatmap. *Nucleic Acids Res.* **43**, W566–W570 (2015).
54. Bay, V. et al. 16S rRNA amplicon sequencing reveals a polymicrobial nature of complicated claw horn disruption lesions and interdigital phlegmon in dairy cattle. *Sci. Rep.* **8**, 15529 (2018).
55. Bay, V., Gür, S. & Bayraktar, O. Plant-derived tormentic acid alters the gut microbiota of the silkworm (*Bombyx mori*). *Sci. Rep.* **12**, 13005 (2022).
56. Fontana, R. & Della Torre, S. The deep correlation between energy metabolism and reproduction: a view on the effects of nutrition for women fertility. *Nutrients* **8**, 87 (2016).

57. Hu, J., Xu, W., Yang, H. & Mu, L. Uric acid participating in female reproductive disorders: a review. *Reprod. Biol. Endocrinol.* **19**, 1–11 (2021).

58. Fabozzi, G. et al. Personalized Nutrition in the management of female infertility: New insights on Chronic Low-Grade inflammation. *Nutrients* **14**, 1–41 (2022).

59. Wu, R. R. et al. Metformin treatment of antipsychotic-induced dyslipidemia: an analysis of two randomized, placebo-controlled trials. *Mol. Psychiatry* **21**, 1537–1544 (2016).

60. Ramos, V. W., Batista, L. O. & Albuquerque, K. T. Effects of fructose consumption on food intake and biochemical and body parameters in Wistar rats. *Revista Portuguesa De Cardiologia: orgao oficial da Sociedade Portuguesa de Cardiologia = Portuguese J. Cardiol. : Official J. Portuguese Soc. Cardiol.* **36**, 937–941 (2017).

61. Gambaro, S. E. et al. M1 macrophage subtypes activation and adipocyte dysfunction worsen during prolonged consumption of a fructose-rich diet. *J. Nutr. Biochem.* **61**, 173–182 (2018).

62. Chan, A. M. L. et al. Recent developments in rodent models of high-fructose diet-induced metabolic syndrome: a systematic review. *Nutrients* **13**, 1–21 (2021).

63. Gunawan, S., Aulia, A. & Soetikno, V. Development of rat metabolic syndrome models: a review. *Vet. World.* **14**, 1774–1783 (2021).

64. Pektaş, M. B., Sadi, G. & Akar, F. Long-term dietary fructose causes gender-different metabolic and vascular dysfunction in rats: Modulatory effects of Resveratrol. *Cell. Physiol. Biochem.: Int. J. Exp. Cell. Physiol. Biochem. Pharmacol.* **37**, 1407–1420 (2015).

65. de Lima, L. M. A., Wiernsperger, N., Kraemer-Aguiar, L. G. & Bouskela, E. Short-term treatment with metformin improves the cardiovascular risk profile in first-degree relatives of subjects with type 2 diabetes mellitus who have a metabolic syndrome and normal glucose tolerance without changes in C-reactive protein or fibrinoge. *Clin. (Sao Paulo Brazil)* **64**, 415–420 (2009).

66. Lin, S. H. et al. Effect of metformin monotherapy on serum lipid profile in statin-naïve individuals with newly diagnosed type 2 diabetes mellitus: a cohort study. *PeerJ* **6**, e4578 (2018).

67. Kamenova, P. Therapeutic potential of metformin in normal glucose tolerant persons with metabolic syndrome. *Biotechnol. Biotechnol. Equip.* **34**, 30–37 (2020).

68. Lv, Z. & Guo, Y. Metformin and its benefits for various diseases. *Front. Endocrinol.* **11**, 191 (2020).

69. Burul-Bozkurt, N., Pekiner, C. & Kelicen, P. Diabetes alters aromatase enzyme levels in gonadal tissues of rats. *Naunyn-Schmiedeberg's Arch. Pharmacol.* **382**, 33–41 (2010).

70. Maliqueo, M. et al. Continuous administration of a P450 aromatase inhibitor induces polycystic ovary syndrome with a metabolic and endocrine phenotype in female rats at adult age. *Endocrinology* **154**, 434–445 (2013).

71. Bertoldo, M. J., Faure, M., Dupont, J. & Froment, P. Impact of metformin on reproductive tissues: an overview from gametogenesis to gestation. *Annals Transl. Med.* **2**, 1–13 (2014).

72. Dean, A., Nilsen, M., Loughlin, L., Salt, I. P. & MacLean, M. R. Metformin reverses development of pulmonary hypertension via aromatase inhibition. *Hypertension.* **68**, 446–454 (2016).

73. El-Attar, A. A., Ibrahim, O. M., Alhassanin, S. A., Essa, E. S. & Mostafa, T. M. Effect of metformin as an adjuvant therapy to letrozole on estradiol and other biomarkers involved in the pathogenesis of breast cancer in overweight and obese postmenopausal women: a pilot study. *Eur. J. Clin. Pharmacol.* **79**, 299–309 (2023).

74. Petersen, M. C. & Shulman, G. I. Mechanisms of insulin action and insulin resistance. *Physiol. Rev.* **98**, 2133–2223 (2018).

75. Lee, E. R. et al. Interplay between PI3K/Akt and MAPK signaling pathways in DNA-damaging drug-induced apoptosis. *Biochim. et Biophys. Acta - Mol. Cell. Res.* **1763**, 958–968 (2006).

76. Yue, J. & López, J. M. Understanding MAPK signaling pathways in apoptosis. *Int. J. Mol. Sci.* **21**, 2346 (2020).

77. Dupont, J. & Scaramuzzi, R. J. Insulin signalling and glucose transport in the ovary and ovarian function during the ovarian cycle. *Biochem. J.* **473**, 1483–1501 (2016).

78. Burks, D. J. et al. IRS-2 pathways integrate female reproduction and energy homeostasis. *Nature* **407**, 377–382 (2000).

79. Lei, L. et al. IRS2 depletion inhibits cell proliferation and decreases hormone secretion in mouse granulosa cells. *J. Reprod. Dev.* **64**, 409–416 (2018).

80. Akamine, E. H. et al. Obesity induced by high-fat diet promotes insulin resistance in the ovary. *J. Endocrinol.* **206**, 65–74 (2010).

81. Liu, M., Zhu, H., Zhu, Y. & Hu, X. Guizhi Fuling Wan reduces autophagy of granulosa cell in rats with polycystic ovary syndrome via restoring the PI3K/AKT/mTOR signaling pathway. *J. Ethnopharmacol.* **270**, 113821 (2021).

82. Wallach, E. E., Barbieri, R. L., Smith, S. & Ryan, K. J. The role of hyperinsulinemia in the pathogenesis of ovarian hyperandrogenism. *Fertil. Steril.* **50**, 197–212 (1988).

83. Wang, J., Wu, D., Guo, H. & Li, M. Hyperandrogenemia and insulin resistance: the chief culprit of polycystic ovary syndrome. *Life Sci.* **236**, 116940 (2019).

84. Kolodziejczyk, B., Duleba, A. J., Spaczynski, R. Z. & Pawelczyk, L. Metformin therapy decreases hyperandrogenism and hyperinsulinemia in women with polycystic ovary syndrome. *Fertil. Steril.* **73**, 1149–1154 (2000).

85. Tao, X., Cai, L., Chen, L., Ge, S. & Deng, X. Effects of metformin and Exenatide on insulin resistance and AMPKα-SIRT1 molecular pathway in PCOS rats. *J. Ovarian Res.* **12**, 86 (2019).

86. Xu, B. et al. Metformin ameliorates polycystic ovary syndrome in a rat model by decreasing excessive autophagy in ovarian granulosa cells *via* the PI3K/AKT/mTOR pathway. *Endocr. J.* **69**, 863–875 (2022).

87. Demirel, M. A. et al. Therapeutic effects of resveratrol in Escherichia coli-induced rat endometritis model. *Naunyn-Schmiedeberg's Arch. Pharmacol.* **392**, 1577–1589 (2019).

88. Sanchez-Garrido, M. A. & Tena-Sempere, M. Metabolic dysfunction in polycystic ovary syndrome: pathogenic role of androgen excess and potential therapeutic strategies. *Mol. Metabol.* **35**, 100937 (2020).

89. Chen, W. & Pang, Y. Metabolic syndrome and PCOS: Pathogenesis and the role of metabolites. *Metabolites* **11**, 869 (2021).

90. Mirzaei, R., Bidgoli, S. A., Khosrokhavar, R., Shoeibi, S. & Ashtiani, H. A. Increased risk of primary ovarian insufficiency by high-fructose diet consumption: a 90-day study in female rats. *Environ. Sci. Pollut. Res. Int.* **30**, 7415–7426 (2023).

91. Zhao, F., Hu, X. & Ying, C. Advances in Research on the relationship between vaginal microbiota and adverse pregnancy outcomes and Gynecological diseases. *Microorganisms* **11**, 991 (2023).

92. Lee, W. L., Tsui, K. H. & Wang, P. H. Lactobacillus and health. *J. Chin. Med. Assoc.: JCMA* **79**, 639–641 (2016).

93. Villa, P. et al. The interplay between immune system and microbiota in gynecological diseases: a narrative review. *Eur. Rev. Med. Pharmacol. Sci.* **24**, 5676–5690 (2020).

94. Chee, W. J. Y., Chew, S. Y. & Than, L. T. L. Vaginal microbiota and the potential of Lactobacillus derivatives in maintaining vaginal health. *Microb. Cell. Fact.* **19**, 203 (2020).

95. Baker-Austin, C. et al. *Vibrio* spp. infections. *Nat. Rev. Dis. Prim.* **4**, 1–19 (2018).

96. Newton, A., Kendall, M., Vugia, D. J., Henao, O. L. & Mahon, B. E. Increasing rates of vibriosis in the United States, 1996–2010: review of surveillance data from 2 systems. *Clin. Infect. Dis.* **54**, S391–S395 (2012).

97. Howard-Jones, N. Robert Koch and the cholera vibrio: a centenary. *Br. Med. J. (Clin. Res. Ed.).* **288**, 379 (1984).

98. Altekruse, S. F. et al. Vibrio gastroenteritis in the US Gulf of Mexico region: the role of raw oysters. *Epidemiol. Infect.* **124**, 489–495 (2000).

99. Letchumanan, V., Chan, K. G. & Lee, L. H. Vibrio parahaemolyticus: a review on the pathogenesis, prevalence, and advance molecular identification techniques. *Front. Microbiol.* **5**, 705 (2014).

100. Hall, V. Actinomyces-gathering evidence of human colonization and infection. *Anaerobe* **14**, 1–7 (2008).

101. Könönen, E. & Wade, W. G. Actinomyces and related organisms in human infections. *Clin. Microbiol. Rev.* **28**, 419–442 (2015).

102. Smego, R. A. Jr. & Foglia, G. Actinomycosis *Clin. Infect. Dis.* **26**, 1255–1261 (1998).
103. Biddle, A., Stewart, L., Blanchard, J. & Leschine, S. Untangling the genetic basis of Fibrolytic specialization by Lachnospiraceae and Ruminococcaceae in Diverse Gut communities. *Diversity* **5**, 627–640 (2013).
104. Campbell, S. C. et al. The effect of diet and exercise on intestinal integrity and microbial diversity in mice. *PLOS ONE* **11**, e0150502 (2016).
105. Zhang, J. et al. Beneficial effect of butyrate-producing Lachnospiraceae on stress-induced visceral hypersensitivity in rats. *J. Gastroenterol. Hepatol. (Australia)* **34**, 1368–1376 (2019).
106. Balakrishnan, B. et al. Prevotella histicola protects from arthritis by expansion of allobaculum and augmenting butyrate production in humanized mice. *Front. Immunol.* **12**, 609644 (2021).
107. Yang, J. et al. Oscillospira-a candidate for the next-generation probiotics. *Gut Microbes* **13**, 1987783 (2021).
108. Chayanupatkul, M. et al. Probiotics and their beneficial effects on alcohol-induced liver injury in a rat model: the role of fecal microbiota. *BMC Complement. Med. Ther.* **22**, 168 (2022).
109. Konikoff, T. & Gophna, U. Oscillospira: a Central, enigmatic component of the human gut microbiota. *Trends Microbiol.* **24**, 523–524 (2016).
110. Waters, J. L. & Ley, R. E. The human gut bacteria Christensenellaceae are widespread, heritable, and associated with health. *BMC Biol.* **17**, 83 (2019).
111. Li, X. et al. Regional distribution of Christensenellaceae and its associations with metabolic syndrome based on a population-level analysis. *PeerJ* **8**, e9591 (2020).
112. Coello, K. et al. Affective disorders impact prevalence of Flavonifractor and abundance of Christensenellaceae in gut microbiota. *Prog. Neuropsychopharmacol. Biol. Psychiatry* **110**, 110300 (2021).
113. Tavella, T. et al. Elevated gut microbiome abundance of Christensenellaceae, Porphyromonadaceae and Rikenellaceae is associated with reduced visceral adipose tissue and healthier metabolic profile in Italian elderly. *Gut Microbes* **13**, 1880221 (2021).

Acknowledgements

Author contributions

MAD, FA, and MOU designed the study. MAD and ES performed the in vivo study. IHO performed the histopathological analysis. KS, MT, OEDK performed Western blot and PCR analyses. VB prepared bioinformatic results. MAD and ES analyzed the data. MAD, FA, ES, VB, MT, and IHO wrote the manuscript.

Competing interests

The authors declare no competing interests.

Additional information

Supplementary Information The online version contains supplementary material available at https://doi.org/10.1038/s41598-024-76211-5.

Correspondence and requests for materials should be addressed to M.A.D.

Reprints and permissions information is available at www.nature.com/reprints.

Publisher's note Springer Nature remains neutral with regard to jurisdictional claims in published maps and institutional affiliations.